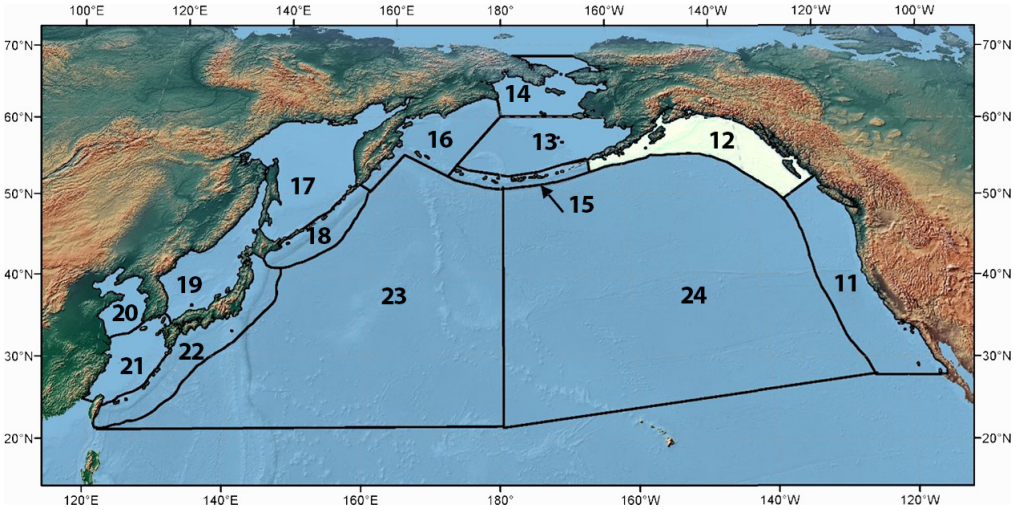

PICES

Regional Report for PICES Region: 12

PICES SPECIAL PUBLICATION 7

Marine Ecosystems of the North Pacific Ocean 2009–2016

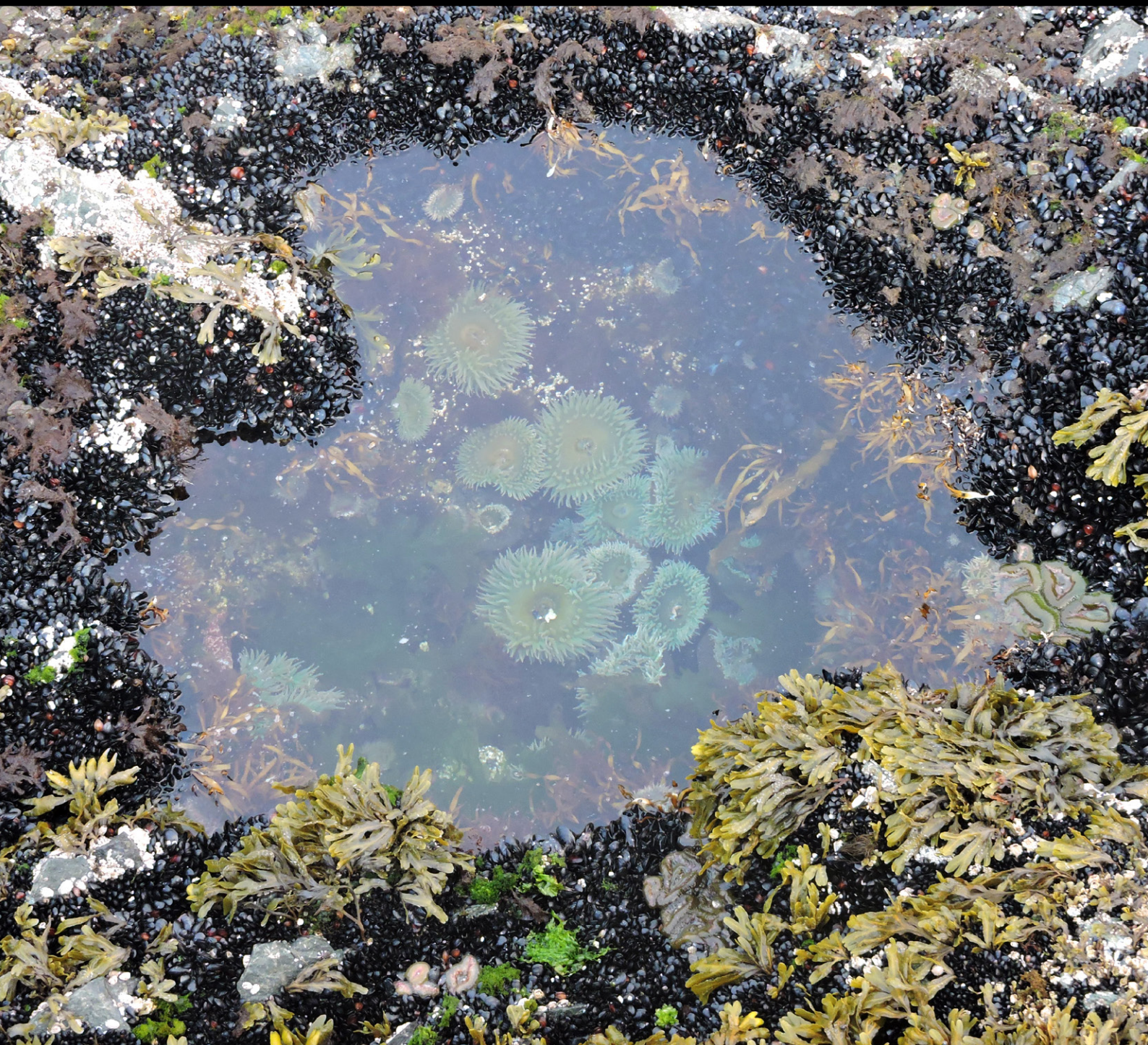

PICES North Pacific Ecosystem Status Report, Region 12

(Gulf of Alaska System)

Stephani Zador and Stephen Kasperski

Nicholas Bond, William Stockhausen, Steve Barbeaux, Seth Danielson, Russell Hopcroft, Peter Chandler, Suzanne Strom, Kathy Kuletz, Sonia Batten, Kenneth Coyle, Lauren Rogers, Alison Deary, Kathryn Mier, Andy Whitehouse, Sarah Gaichas, Chris Rooper, Franz Mueter, Jennifer Boldt, Jerry Hoff, Gregory Ruggerone, Jim Irvine, Heather Renner, Nora Rojek, Arthur Kettle, Brie Drummond, Katie Sweeney, Tom Gelatt, K. Savage, John Elliott, Aroha Miller, Kyle Elliott, Sandi Lee

1. Highlights

The main physical oceanographic highlights for the decade 2009–2018 include a predominantly cold period from 2007–2013 and a marine heatwave from 2014–2016. During the predominantly cold period, biological ecosystem components known to be more productive during cold periods followed the expected pattern. For example, capelin (*Mallotus villosus*) abundance increased.

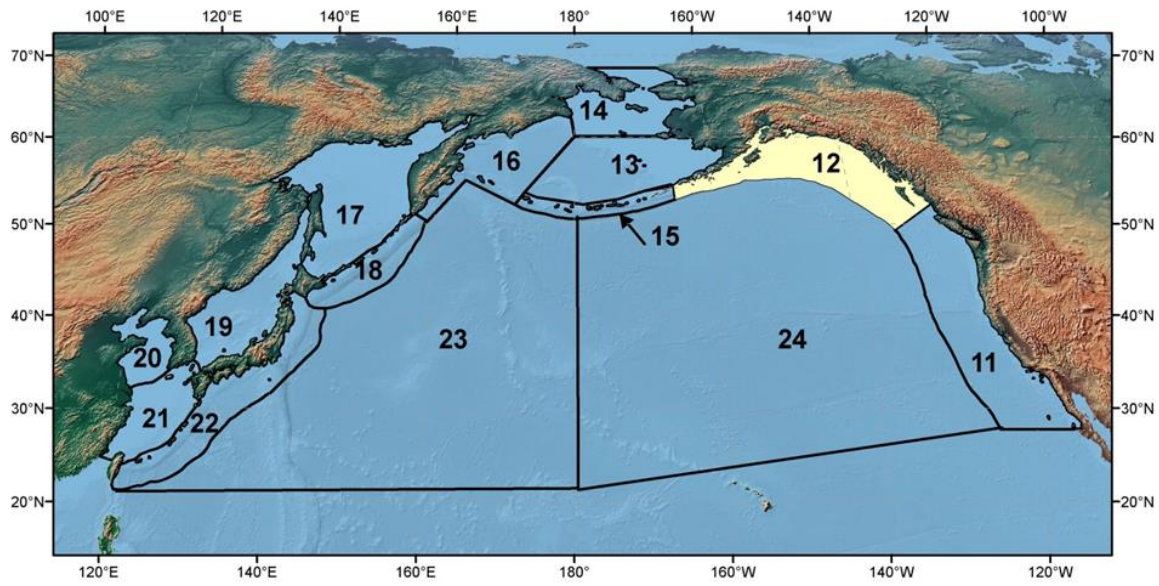

Figure R12- 1. The PICES biogeographical regions and naming convention for the North Pacific Ocean with the area discussed in this report **are** highlighted

Biological indicators highlighted poor productivity across many trophic levels in 2011, but the physical origins of this response remain unclear. Many physical indicators expressed a marked change in sign in 2014 when the heatwave began, but many biological indicators remained in productive states. While the physical indicators remained unchanged in 2015, biological indicators began to show impacts. The timing of the lagged biological responses varied across species and trophic levels. Notable biological impacts include extensive seabird and whale die-offs and an 80% decline in the Gulf of Alaska Pacific cod (*Gadus macrocephalus*) stock.

2. Introduction

This chapter updates pelagic ecosystem indicators for the Gulf of Alaska large marine ecosystem (PICES Region 12), focusing on the decade 2009–2018. Some indicators were selected from those that were submitted through the PICES Submittables ETSO process (identified herein as ETSO). Many indicators were selected from those contributed to the annual Gulf of Alaska Ecosystem Status Reports produced by the Alaska Fisheries Science Center, NOAA, for the North Pacific Fisheries Management Council (identified herein as GOA ESR). Other indicators were derived from publicly available datasets. Lead scientists/contributors and sources are noted for each indicator topic. Text is excerpted from the ETSOs and ESRs.

3. Atmosphere

3.1. Climate Indices

Investigator(s): Nicholas Bond
Joint Institute for the Study of the Atmosphere and Ocean (JISAO)
Source: GOA ESR 2018, ETSO

NINO3.4 – This index represents the normalized SST anomalies in the east-central tropical Pacific (5˚S – 5˚N; 170 -120˚W) and is used to summarize the state of the El Nino-Southern Oscillation (ENSO). Positive values of +1 and greater signify El Nino events; negative values signify La Nina. ENSO neutral conditions are assumed to be present when the magnitude of NINO3.4 is less than 0.5 to 1, depending on the application and averaging period. ENSO generally has its strongest expression during the boreal winter, which is also the time of year when it has more robust connections to the atmospheric circulation of the North Pacific Ocean. El Nino and La Nina events tend to be accompanied by relatively low and high sea level pressure (SLP), respectively, in the vicinity of the Aleutian low. The time series provided here is a seasonal (November through March) average of NINO3.4 monthly anomaly values in ˚C (the year refers to that for the months of January through March). This time series was produced using the web application at https://www.esrl.noaa.gov/psd/dat/climateindices/ based on data compiled by NOAA/Climate Prediction Center. Users of NINO3.4 and other SST-based climate indices should be aware that different SST analyses yield slightly different values for these indices. In addition, there are a host of ENSO indices with a variety of atmospheric and oceanic

variables as inputs. The discrepancies between ENSO indices are usually minor with respect to characterization of the major fluctuations in ENSO.

Trends: ENSO exhibits periodicity on time scales typically of 2 to 7 years (Figure R12-2). The period of interest here (2009 into 2016) featured the following prominent events: a moderately strong El Nino during the boreal winter of 2009-2010, La Nina conditions during the winter of 2010-11, and to a lesser extent during the winter of 2011-12, and an intense El Nino that developed during summer 2015 and persisted into the spring of 2016. The tropical Pacific was also warmer than normal during the previous winter of 2014-15; in some classification systems it qualifies as an El Nino winter and in others, it does not. Similarly, the tropical Pacific was cooler than normal during fall 2016, representing a borderline La Nina state.

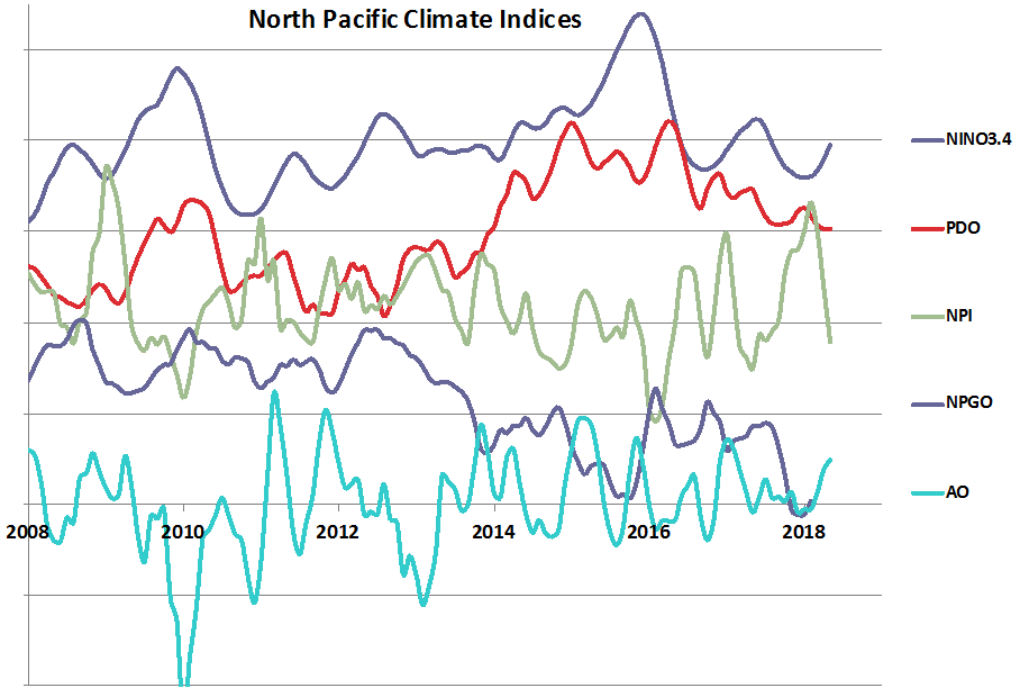

Figure R12-2. Climate indices relevant to the Gulf of Alaska: NINO3.4, Pacific Decadal Oscillation (PDO), North Pacific Index (NPI), North Pacific Gyre Oscillation (NPGO) and Arctic Oscillation (AO).

Pacific Decadal Oscillation (PDO) – The PDO represents the leading mode of variability in North Pacific SST. It was first related to western North America salmon catches (Mantua et al. 1997) and since been linked to a host of marine ecosystem variations. The PDO responds to the strength of the Aleutian low (Newman et al. 2016), with upper-ocean processes and thermal inertia serving to low-pass filter the atmospheric forcing. Monthly values of the PDO in normalized form are available at the following website: http://research.jisao.washington.edu/pdo/PDO.latest.txt. These data were used to form the annual averages included here.

Trends: The PDO was in a mostly negative state from 2008 through 2013, with a short period of weakly positive values from late 2009 into 2010 (the annual averaged PDO for these two years was less than zero) (Figure R12-2). A marked shift in the PDO began in late 2013 with positive values for this index prevailing from 2014 through 2016. This increase can be attributed initially

to the development of the NE Pacific marine heat wave of 2014-16, and was reinforced by the atmospheric forcing associated with El Nino during the winter of 2015-16, in particular, a deeper than normal Aleutian low.

North Pacific Index (NPI) – The NPI is used to characterize the strength of the Aleutian low, specifically the area-weighted sea level pressure (SLP) in hPa over the region of 30 - 65˚N, 160˚E – 140˚W (Trenberth and Hurrell 1994). It appears to be most valuable as an atmospheric circulation index during the boreal winter; yearly values of November through March averages are provided here. El Nino and La Nina events tend to be accompanied by relatively low and high SLP, respectively, in the vicinity of the Aleutian low, as reflected by the NPI. The seasonal mean NPI time series contained herein was produced by the same application as was used for the NINO3.4 index (https://www.esrl.noaa.gov/psd/dat/climateindices/).

Trends: The NPI is an atmospheric index and therefore has inherently greater high-frequency variability than most oceanic indices (Figure R12-2). The winter averages provided here range from strongly positive values for 2008-09 to moderately negative values for the winters of 2009-10 and 2015-16, each of which featured El Nino. Note that the former event was substantially weaker than the latter event as gauged by the NINO3.4 index, but that the remote atmospheric responses in terms of the NPI were comparable. The NPI was positive for the winters of 2009-10 through 2013-14 during a period that included mostly negative states for the NINO3.4 and PDO indices.

North Pacific Gyre Oscillation (NPGO) – The NPGO represents the second leading mode of sea surface height (SSH) variability in the North Pacific. Di Lorenzo et al. (2008, among later articles) have shown that the NPGO is related to a variety of physical and biochemical ocean variables in the eastern North Pacific. The NPGO has also been related to zooplankton species composition in the western North Pacific (Chiba et al. 2013). Annual averages were formed from the monthly values of the NPGO in normalized form downloaded from the following website: http://www.o3d.org/npgo/.

Trends: Positive values of the NPGO prevailed from 2009 through most of 2013, implying relatively cool SST across the North Pacific north of about 40 N and warm SST in the western North Pacific south of 40°N (Figure R12-2). The NPGO shifted to a negative state in late 2013, with this state persisting through 2015. This period coincides with relatively warm upper ocean temperatures in much of the northeast Pacific. The NPGO was near zero for 2016 as a whole.

4. Physical Ocean

4.1. PAPA Trajectory Index

Investigator(s): William Stockhausen
NOAA, Alaska Fisheries Science Center
Source: GOA ESR 2018

Methods: The PAPA Trajectory Index (PTI) provides an annual index of near-surface water movement variability, based on the trajectory of a simulated surface drifter released at Ocean Station PAPA (50°N, 145°W) The simulation for each year is conducted using the “Ocean

Surface CURrent Simulator" (OSCURS; http://oceanview.pfeg.noaa.gov/oscurs). Using daily gridded atmospheric pressure fields, OSCURS calculates the speed and direction of water movement at the ocean's surface at the location of a simulated surface drifter. It uses this information to update the position of the simulated drifter on a daily basis over a specified time period. For the index presented here, OSCURS was run for 90 days to simulate a surface drifter released at Ocean Station PAPA on December 1 for each year from 1901 to 2017 (trajectory endpoints years-1902 to 2018).

Individual trajectories reflect interannual variability in regional (northeast Pacific) wind patterns which drive short-term changes in ocean surface currents, as well as longer term changes in atmospheric forcing that influence oceanic current patterns on decadal time scales (Figure R12-3). Filtered PTI values greater than the long-term mean are indicative of increased transport and/or a northerly shift in the Alaska Current, which transports warm water northward along the west coast of Canada and southeast Alaska from the south and consequently plays a major role in the Gulf of Alaska's heat budget.

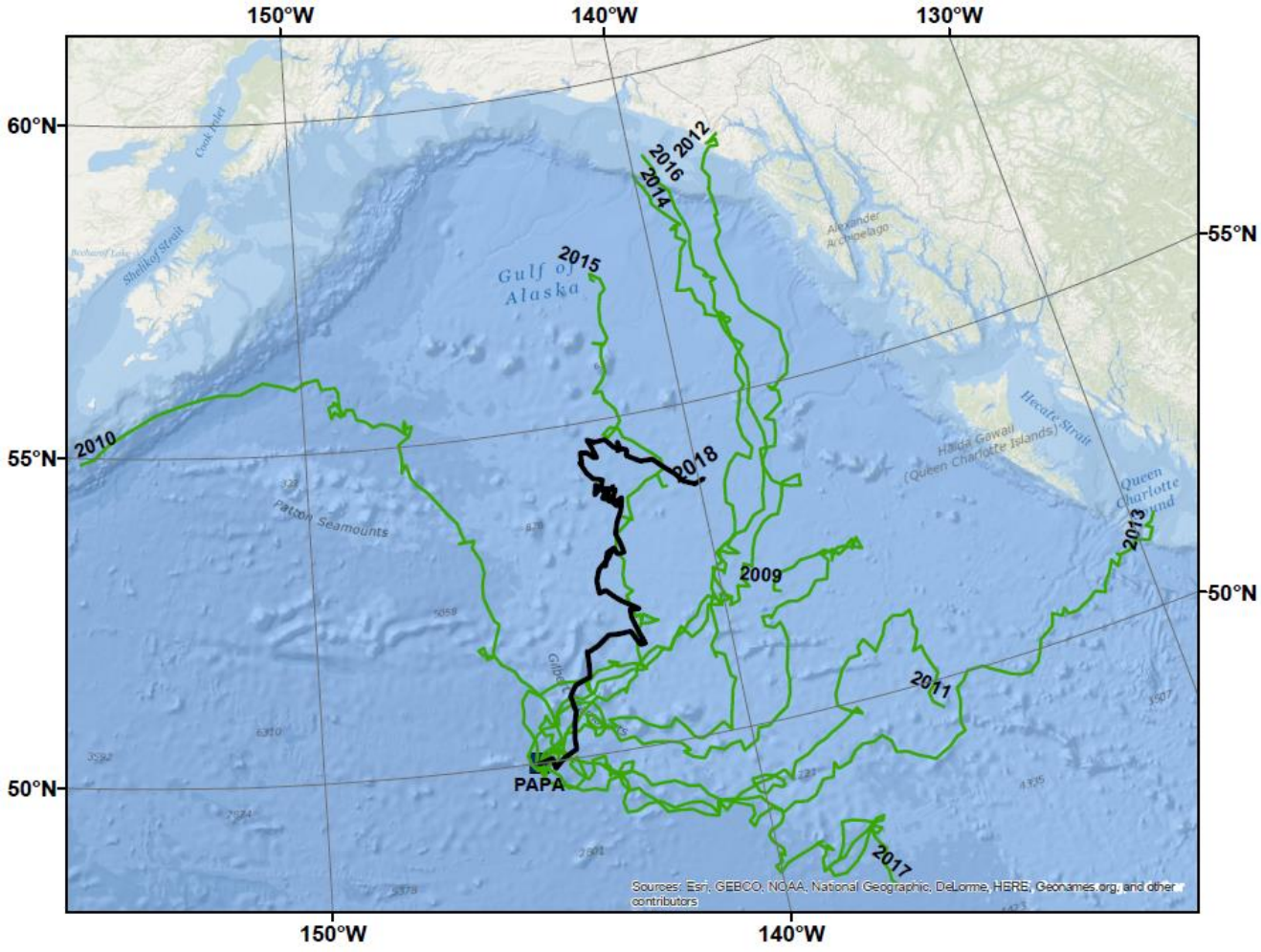

Figure R12-3. PAPA Trajectory Index simulating drift patterns from December 1st of each year. The year shown is the year at the end of the 90-day simulation.

Trends: Over the past century, the filtered (5-year running average) PTI has undergone four complete oscillations with distinct crossings of the mean, although the durations of the oscillations are not identical: 26 years (1904-1930), 17 years (1930-1947), 17 years (1947-1964), and 41 years (1964-2005) (Figure R12-4). The filtered index indicates that a shift occurred in the mid-2000s to predominantly southerly anomalous flow following a 20+ year period of predominantly northerly anomalous flow. This was indicative of a return to conditions (at least in terms of surface drift) similar to those prior to the 1977 environmental regime shift. This part of the cycle apparently ended rather quickly, however, as it now appears the PTI has crossed the mean in the opposite direction. The recent period of predominantly southern flow has been the shortest and weakest in the time series.

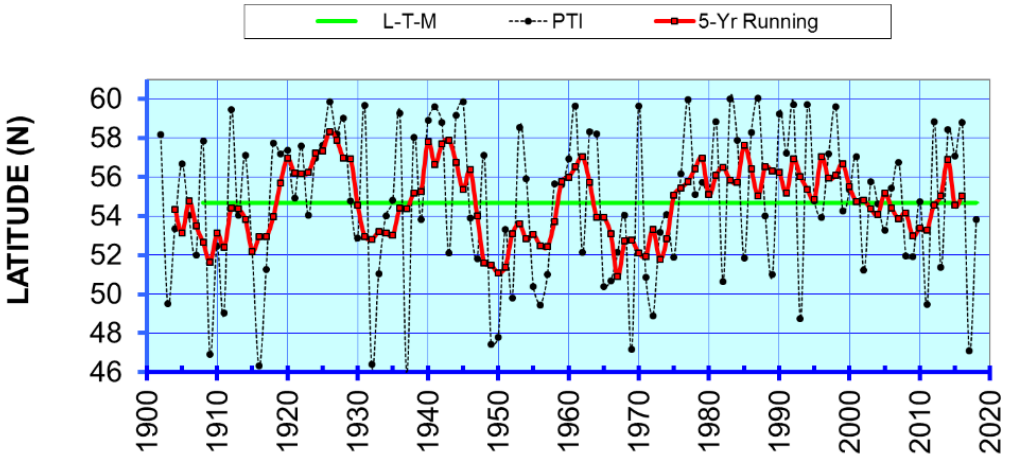

Figure R12-4. PAPA Trajectory Index (PTI) end-point latitudes, winters 1902-2018.

4.2. Marine Heatwave Index

Investigator(s): Steve Barbeaux
NOAA, Alaska Fisheries Science Center
Source: GOA ESR 2018, direct from the author

Methods: The daily sea surface temperatures for 1981 through December 2018 were retrieved from the NOAA High-resolution Blended Analysis Data database (NOAA 2017) and filtered to only include data from the central GOA between 145°W and 160°W longitude for waters less than 300m in depth. The overall daily mean sea surface temperature was then calculated for the entire region. These daily mean sea surface temperatures data were processed through the R package heatwaveR (Schlegel and Smit 2018) to obtain the marine heatwave cumulative intensity (MHWCI; Hobday et al. 2016) value where we defined a heat wave as 5 days or more with daily mean sea surface temperatures greater than the 90th percentile of the 1 January 1983 through 31 December 2012 time series. Data are presented here relative to the upper 90th percentile.

Trends: The Gulf of Alaska was in an extreme marine heatwave (as defined by Hobday et al., 2016) from mid-2014 through the end of 2016 (Figure R12-5). The Gulf of Alaska experienced

heatwaves during 1997/1998 and periodically from 2003 – 2006. Heatwave conditions developed again in late 2018.

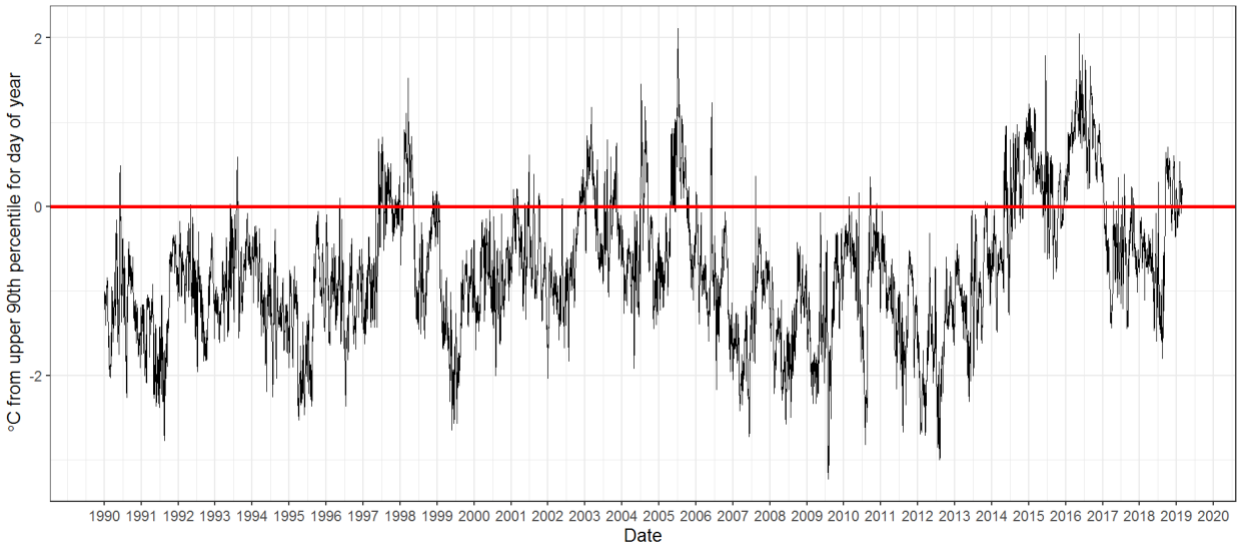

Figure R12-5. Marine heatwave cumulative intensity index anomalies from 1990 to 2019 depicted relative to the upper 90th percentile.

4.3 Temperatures at GAK1

Investigator(s): Seth Danielson, Russell Hopcroft
University of Alaska
Source: GOA ESR 2018, ETSO

Methods: Hydrographic transects have been completed south of Seward Alaska typically during the first 10 days of May for over two decades, 1998-2018 (Figure R12-6). Temperature data are averaged over the top 100m of the water column to provide an index of the heat on the northern Gulf of Alaska shelf that is not biased by short-term weather as are satellites.

Trends: Temperatures have returned to long-term (21 year) means during 2017 and 2018 at stations along the Seward Line (Figure R12-7). The northernmost station, GAK1, that has been occupied for nearly 50 years show long-term warming of the Gulf of Alaska Coastal Current (Figure R12-8). The Seward Line temperatures highlight events such as El Nino's that have occurred across the shelf during 1998, 2003, and 2016, as well as the marine heatwave during 2014-2016.

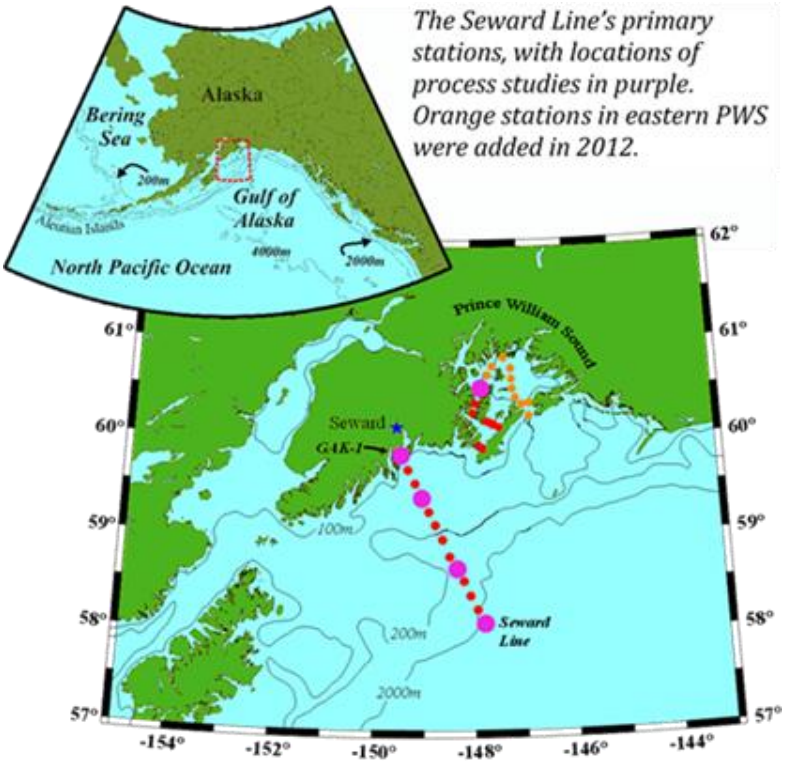

Figure R12-6. The Seward Line monitoring stations in the northern Gulf of Alaska, with the station GAK1 located closest to shore.

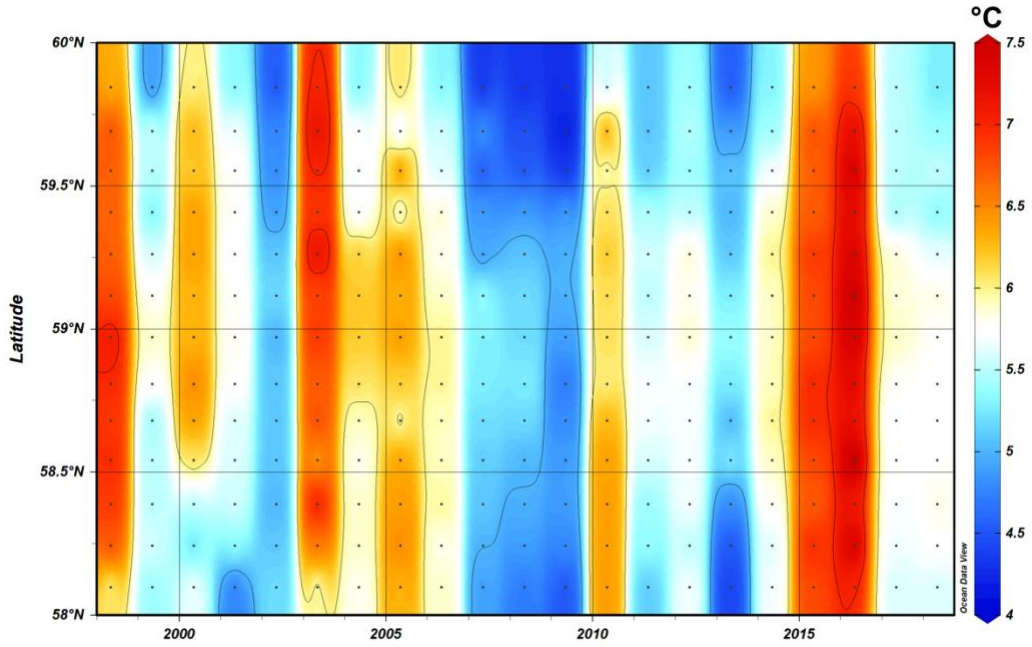

Figure R12-7. Depth-averaged temperatures to 100m during May along the Seward Line.

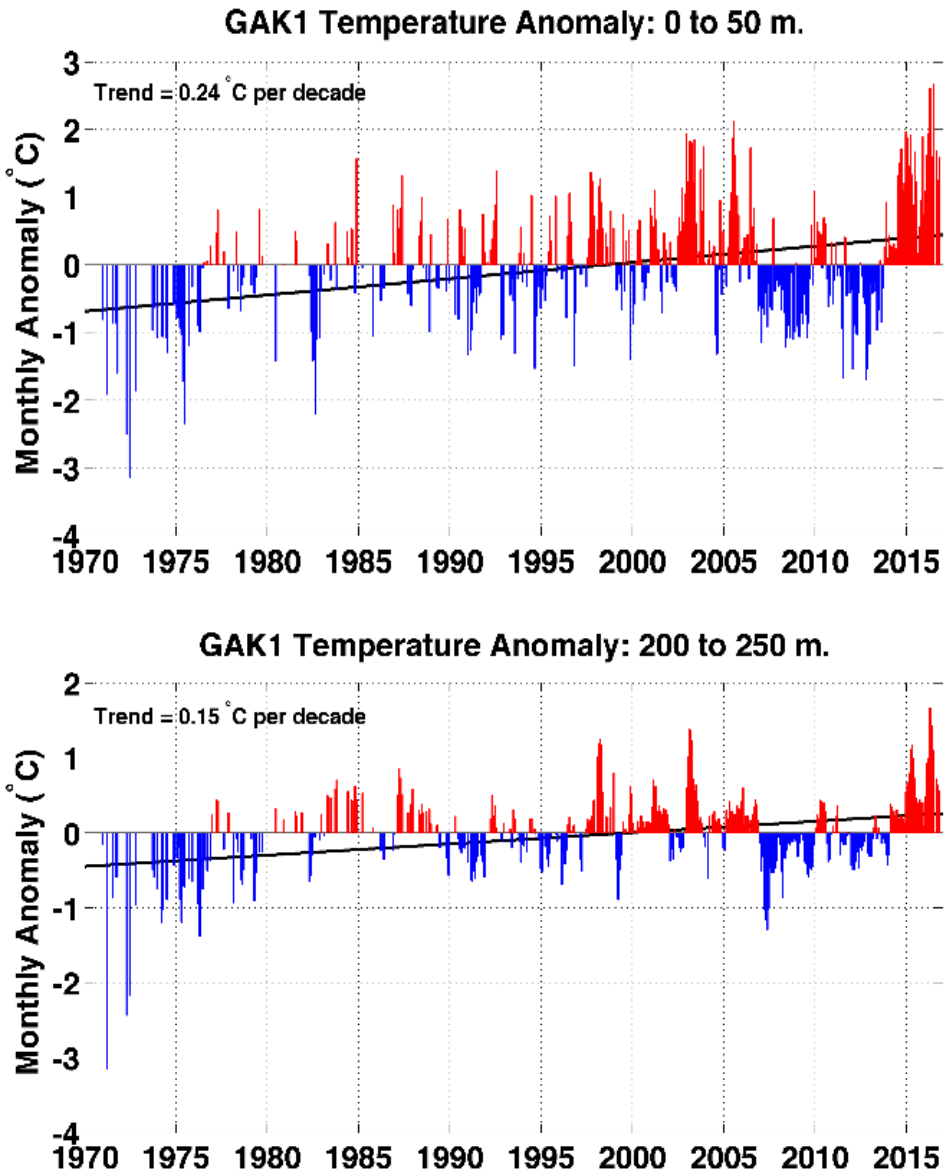

Figure R12-8. Depth-integrated temperatures at GAK1 station near the surface (top figure) and at depth (bottom figure).

4.4. Mixed Layer Depth

Investigator(s): Peter Chandler
Source: ETSO

Methods: The global Argo temperature and salinity profiles are provided by the China Argo Real-time Data Center (http://www.argo.org.cn). Argo data collected before 2004 are not included due to insufficient global coverage of the samples. All of the data have been quality controlled (either a real-time quality control (QC) or a delayed-mode QC) at the national Argo Data Assembly Centers (DACs). Users can refer to the Argo data management documentation

(Wong et al., 2015, Argo quality control manual for CTD and trajectory data Version 3.0, http://dx.doi.org/10.13155/33951) for details.

The Mixed Layer Depth (MLD) for each Argo profile is calculated (Chu et al. 1999) and the corresponding sea surface temperature and salinity are estimated using the linear fitting method in the mixed layer. The initial background state is constructed using Cressman successive correction. The Barnes successive correction is then applied to construct the monthly Argo temperature and salinity grid data from January 2004 to December 2017.

Dataset: BOA_Argo.

Temporal coverage: From January 2004 to December 2017.
Temporal resolution: Monthly.
Spatial resolution:
Horizontal 1°×1° (Longitude: 0.5:1.0:359.5, Latitude: -79.5:1.0:79.5),
Vertical: 58 levels in vertical from surface to 1975 dbar depth.
Author： China Argo Real-time Data Center
Chu, P. C., Q. Q. Wang, R. H. Bourke (1999), A geometric model for Beaufort/Chukchi Sea thermohaline structure. J Atmos OceanTechnol,16:613–632.

Argo data were collected and made freely available by the International Argo Program and the national programs that contribute to it. (http://www.argo.ucsd.edu, http://argo.jcommops.org). The Argo Program is part of the Global Ocean Observing System. "

Trends: Warmer condition was conspicuous after 2014 with 2°C increase compared to the previous period 2008-2013 in both winter and summer SST. The condition persisted through 2018. Less saline condition appeared in 2014 both winter and summer, but salinity returned to the average level in 2017. Interannual variation was detected in winter MLD with weaker mixing in 2013 and 2015, but there was no clear long-term trend. Either no clear interannual variation or long-term trend was observed for summer MLD.

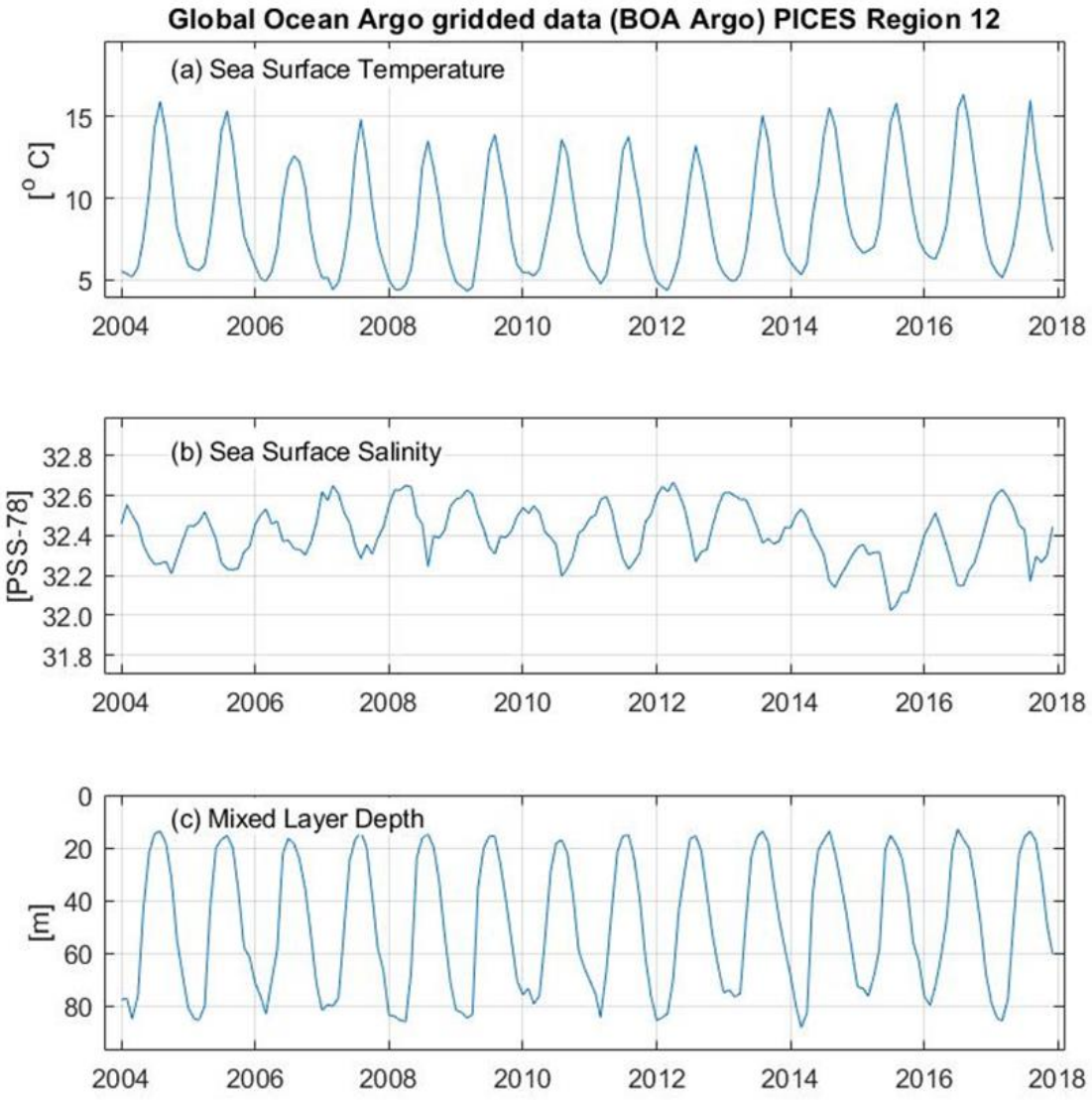

Figure R12-9. Monthly time series of (a) sea surface temperature, (b) sea surface salinity, and (c) Mixed Layer Depth derived from Argo profile data observed in PICES region 12.

5. Phytoplankton

5.1. May Chlorophyll on the Seward Line

Investigator(s): Russell R Hopcroft, Seth L. Danielson, Suzanne L. Strom, Kathy Kuletz
Source: ETSO

Methods: Average integrated May chlorophyll by shelf zone along the Seward Line stations (inner = GAK 1-4; mid = GAK 5-9; outer = GAK 10-13) (see R12-6).

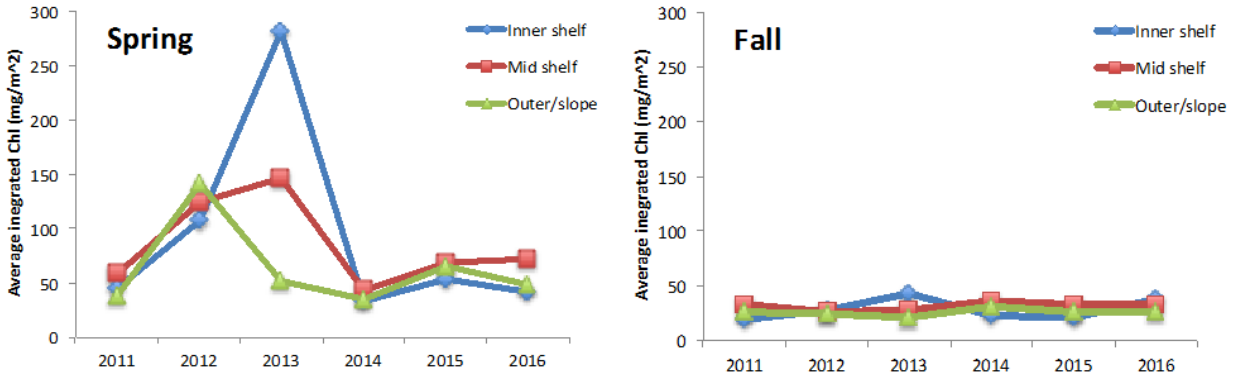

Figure R12-10. Average integrated spring (May) chlorophyll by shelf zone along the Seward Line stations (inner = GAK 1-4; mid = GAK 5-9; outer = GAK 10-13) (see R12-6).

Trends: Macronutrients, phytoplankton (integrated chlorophyll, Fig. R12-10) and microzooplankton time series all show a clear influence of the warmer 2015 and 2016 conditions. During 2013 and 2014, the silicate: nitrate drawdown ratio in surface waters was 1.8, in agreement with the average reported by Strom et al. (2006) for May diatom-dominated communities on the Seward Line during the early 2000s. These nutrient ratios agree with chlorophyll data showing a bloom trajectory by which increases in chlorophyll are associated with increases in large cells (diatoms) on most of the shelf. In the recent warm years, however, silicic acid drawdown associated with spring production is more modest, with an overall silicate: nitrate drawdown ratio of 1.1. This is consistent with the dominance of smaller non-diatom phytoplankton on the shelf in the spring of 2015 and 2016. In addition to these changes in phytoplankton community composition, satellite ocean color data indicate delayed bloom timing and reduced magnitude.

6. Zooplankton

6.1. Mesozooplankton sampled by the Continuous Plankton Recorder

Investigator(s): Sonia Batten
Sir Alastair Hardy Foundation for Ocean Sciences
Source: ETSO, GOA ESR 2018
Methods: The Continuous Plankton Recorder (CPR) is towed behind a commercial ship at a depth of about 7 m. The sampling location in Region 12 is shown in Figure R12-11. The plankton are collected continuously but then sectioned into 18.5 km samples (10 nautical miles), and normally every 4th sample is processed. We identify and count the zooplankton (and larger hard-shelled phytoplankton). After cutting into samples each sample is viewed under a microscope. Twenty fields of view are examined across the sample and taxa are counted as a presence or absence in each. Equivalent numbers of cells per sample are then calculated for 10 levels of abundance (1 or 2 fields = level 1, 3 or 4 fields = level 2 and so on up to 19 or 20 fields = level 10). Taxonomic resolution of zooplankton varies, most copepods are identified to species, certainly to genus, and sometimes to stages.

Trends: The abundance of mesozooplankton was stable from 2008 to 2013 and then increased, so it could also have increased grazing pressure on large diatoms (Figure R12-12 top and middle). The Copepod Size Index showed a slight reduction in size in these years, from a maximum in 2009/10, also consistent with warm conditions favoring smaller species (Figure R12-12 bottom). This pattern was particularly clear in the transect crossing the Alaskan shelf (middle transect of Figure R12-11, which is reflected in anomaly plots of Figure R12-13). The different plankton community of these years, and more, and smaller, zooplankton is likely to have impacts on higher trophic level predators. While mesozooplankton abundance continued to be high after the return to average sea temperatures in 2017, the Copepod Size Index increased.

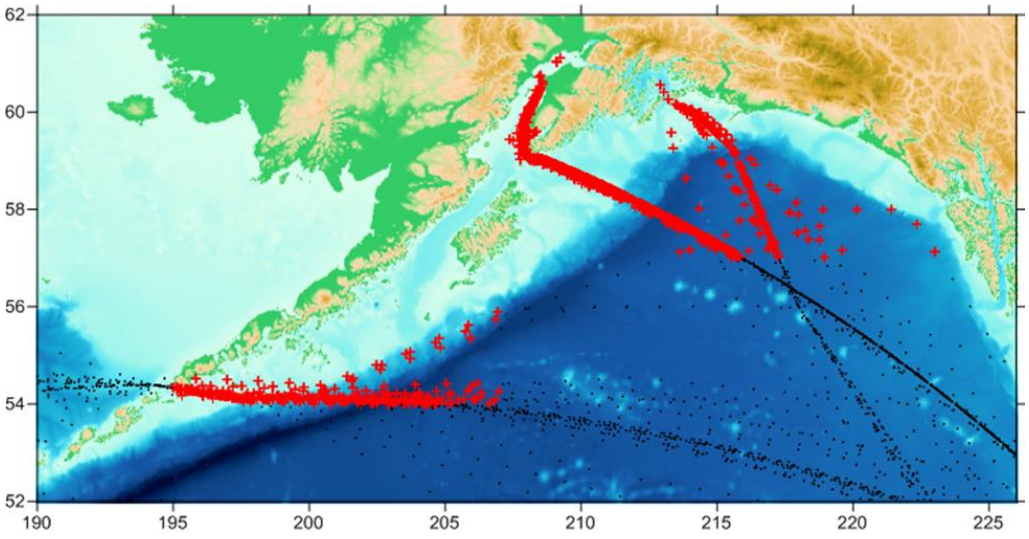

Figure R12-11. Location of CPR samples in Region 12, shown in red. The anomaly plots in Figure R12-13 are based on the portion of the middle transect (going up Cook Inlet) that is over the shelf.

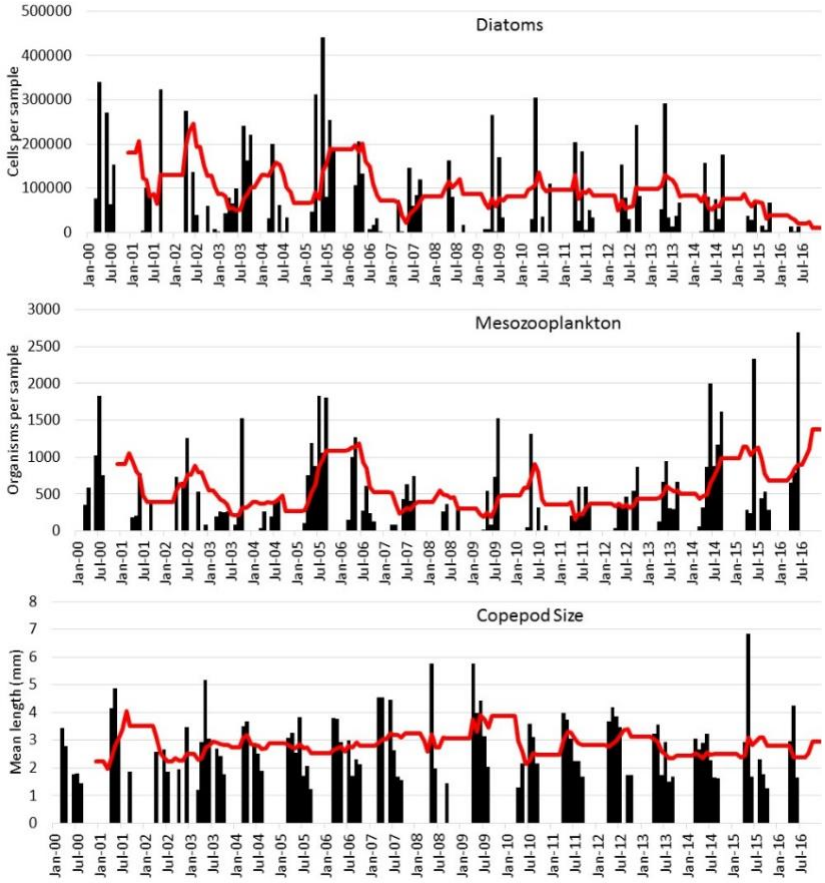

Figure R12-12. Diatom abundance (top) and mesozooplankton abundance (middle) and copepod size index (bottom) based on the CPR Survey. Data for all samples collected in the region per month were averaged to give a monthly mean, presented as black bars. The red line indicates a 12-month running mean to show the long-term trends.

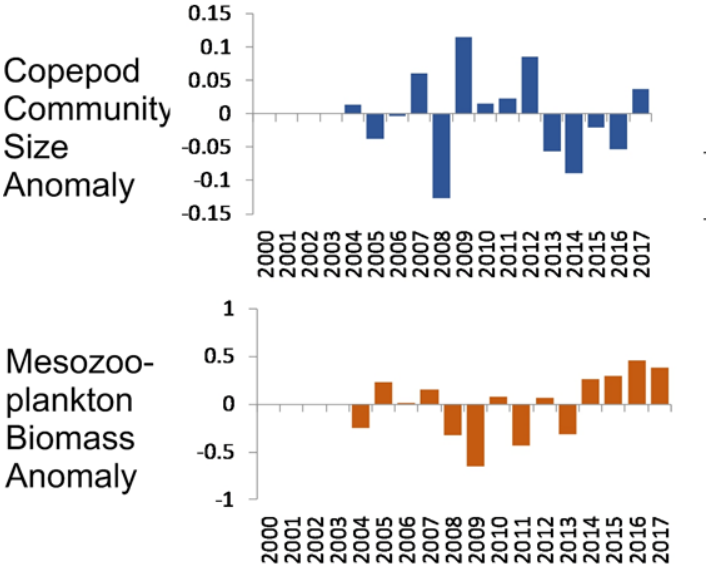

Figure R12-13. Anomaly of Copepod Community Size (top) and mesozooplankton biomass for 2004-2017 based on the CPR survey. Anomaly plots from the over-shelf portion of the middle transect line are depicted in Figure R12-11.

6.2. Spring (May) Large Copepod and Euphausiid Biomass along the Seward Line

Investigator(s): Russell Hopcroft and Kenneth Coyle
University of Alaska
Source: GOA ESR 2018

Methods: Transects have been completed south of Seward Alaska typically during the first 10 days of May for over two decades to determine species composition, abundance, and biomass of the zooplankton community. Data are averaged over the top 100 m of the water column to provide estimates of wet-weight biomass of zooplankton summarized here for all calanoid copepods and euphausiids (a.k.a. krill) retained by a 0.5 mm mesh net. These categories represent key prey for a variety of fish, marine mammals, and seabirds. This project is funded in part by the Gulf Watch Alaska long-term monitoring program funded by the *Exxon Valdez* Oil Spill Trustee Council.

Trends: Large copepod biomass tends to track spring temperatures not because there are more of them, but because they grow faster and therefore individuals are larger when waters are warmer. The warm springs of 2015 and 2016, and their subsequent return to more “typical” temperature appears to have a positive impact on overall community biomass (Figure R12-14 top), although it has significantly altered the mix of species contributing to it. In contrast, euphausiid biomass appears to be negatively impacted by warm springs (Figure R12-14 bottom), with peaks often driven by high abundances of their larval stages when conditions are favorable.

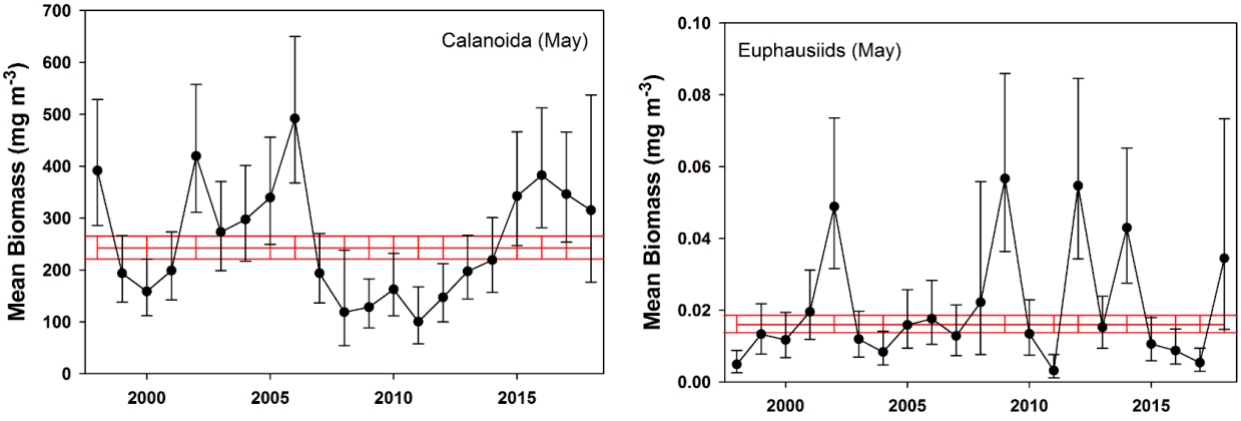

Figure R12-14. Large copepod (left) and euphausiid (right) biomass sampled along the Seward Line. Transect means and 95% confidence intervals (black) are calculated on power-transformed data. Long-term means and their confidence intervals are indicated (red).

6.3. Larval Fish Abundance in the Gulf of Alaska 1981–2017

Investigator(s): Lauren Rogers, Alison Deary, Kathryn Mier
Source: GOA ESR 2018

Methods: The Alaska Fisheries Science Center's (AFSC) Ecosystems and Fisheries Oceanography Coordinated Investigations Program (EcoFOCI) has been sampling ichthyoplankton in the Gulf of Alaska (GOA) from 1972 to the present, with annual sampling from 1981–2011 and biennial sampling during odd-numbered years thereafter. The primary sampling gear used is a 60-cm bongo sampler fitted with 333 or 505-µm mesh nets. Oblique tows are carried out mostly from 100 m depth to the surface or from 10 m off bottom in shallower water (Matarese et al., 2003). Historical sampling has been most intense in the vicinity of Shelikof Strait and Sea Valley during mid-May through early June (Figure R12-15). From this area and time, a subset of data has been developed into time series of ichthyoplankton abundance (after Doyle et al., 2009) for the 12 most abundant larval taxa in the GOA, including commercially and ecologically important species (Figure R12-16). Time series are updated in even years, one year after collection, due to processing time required for quantitative data. On-board counts of a limited number of taxa give rapid assessments of abundance, which are presented in the year of collection.

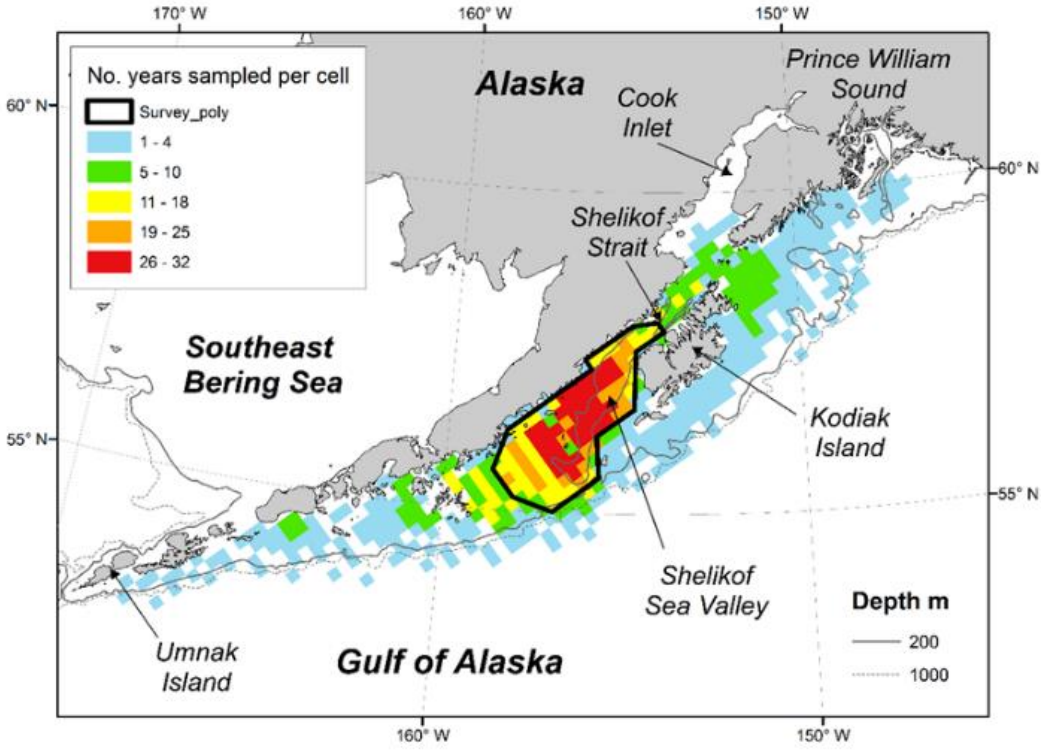

Figure R12-15. Distribution of historical ichthyoplankton sampling in the Gulf of Alaska by NOAA's Alaska Fisheries Science Center using a 60 cm frame bongo net. Sampling effort is illustrated by the number of years where sampling occurred in each 20 km^2 grid cell during late spring. A time series has been developed for the years 1981-2017 from collections in the polygonal area outlined in black where sampling has been most consistent during mid-May through early June. Note that this polygon was updated in 2018 to reflect sampling intensity through the most recent years.

Trends: Abundances for most species have returned towards average levels after the impact of the 2014–2016 marine heatwave in the Gulf of Alaska. Many species, including Pacific cod and walleye pollock, had record low abundances in 2015, which presaged recruitment failures for these stocks. In 2017, walleye pollock larval abundance was above average, as also indicated by on-board rough counts of larvae presented. Pacific cod appear to have recovered somewhat from the low in 2015, but remained below average in 2017. All but three taxa saw an increase in larval abundance from 2015 levels. Larval rockfish departed from the trend of increasing abundance observed since 2007, and declined to the long-term mean. Southern rock sole abundance was anomalously high (second highest on record), and has been increasing, on average, since 2000.

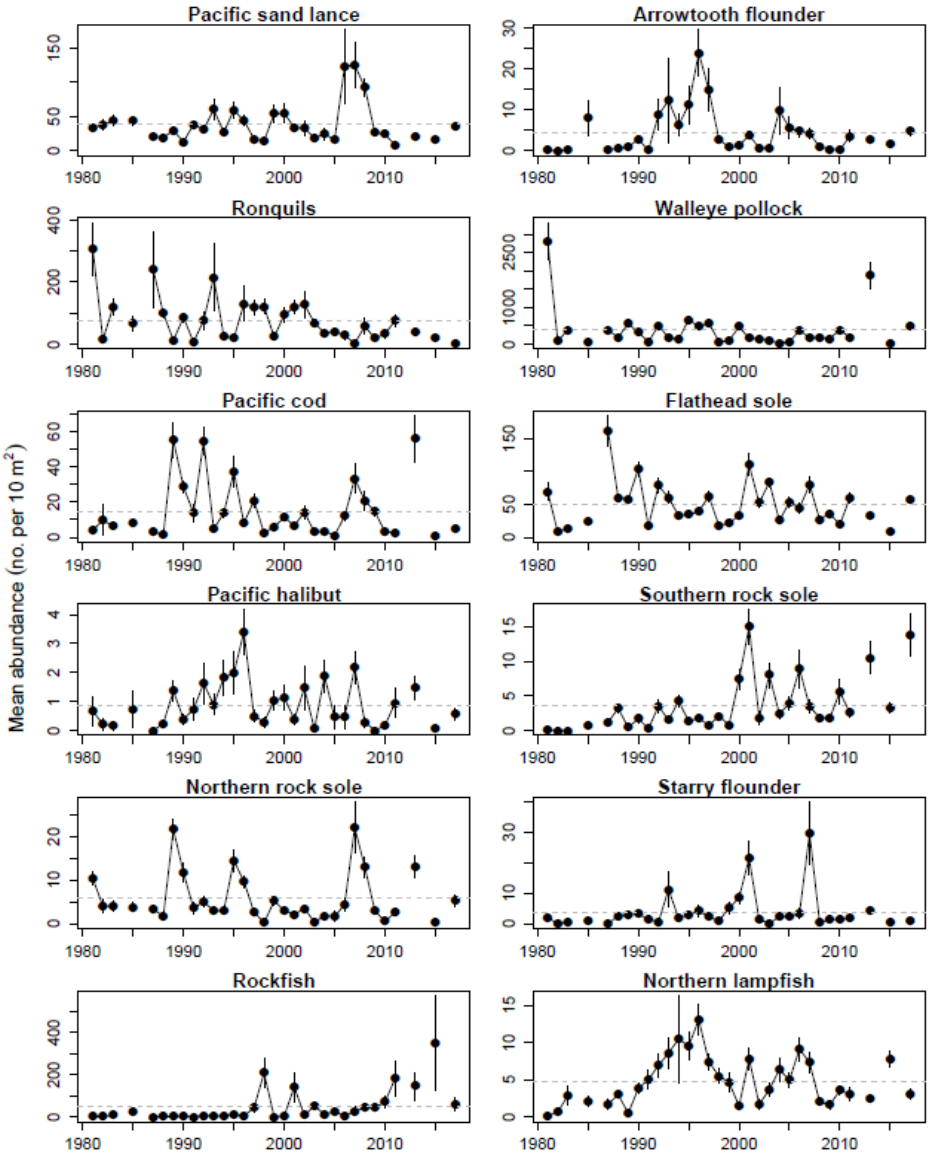

Figure R12-16. Interannual variation in late spring larval fish abundance in the Gulf of Alaska 1981-2017. The larval abundance index is expressed as the mean abundance (no. 10 m^{-2}), and the long-term mean is indicated by the dashed line. Error bars show +/- 1 SE. No data are available for 1984, 1986, 2012, 2014, or 2016.

6.4. Scyphozoan jellyfish caught in commercial groundfish fisheries

Investigator(s): Andy Whitehouse[1], Sarah Gaichas[2], and Stephani Zador[3]
[1] Joint Institute for the Study of the Atmosphere and Ocean (JISAO), [2] NOAA Northeast Fisheries Science Center, [3] NOAA Alaska Fisheries Science Center
Source: GOA ESR 2018

Methods: Total catch of non-target species is estimated from observer species composition samples taken at sea during fishing operations, scaled up to reflect the total catch by both observed and unobserved hauls and vessels operating in all US Fishery Management Plan (FMP) areas. Catch since 2003 has been estimated using the Alaska Region's Catch Accounting System. This sampling and estimation process result in uncertainty in catches, which is greater when observer coverage is lower and for species encountered rarely in the catch.

Trends: The catch of Scyphozoan jellies in the GOA has been variable from 2011-2017, with the highest catch in 2016 (Figure R12-17). Other years of elevated catch were 2012 and 2015 and were preceded by years of reduced catch. The catch in 2017 was the second lowest over this time period. Scyphozoan jellies are primarily caught in the pollock fishery.

The catch of non-target species may change if fisheries management practices and/or ecosystems change. Because non-target species catch is unregulated and unintended, if there have been no large-scale changes in fishery management in a particular ecosystem, then large-scale signals in the non-target catch may indicate ecosystem changes. Catch trends may be driven by changes in biomass or changes in distribution (overlap with the fishery) or both. Fluctuations in the abundance of jellyfish are influenced by a suite of biophysical factors affecting the survival, reproduction, and growth of jellies including temperature, wind-mixing, ocean currents, and prey abundance (Purcell 2005, Brodeur et al. 2008). The lack of a clear trend in the catch of scyphozoan jellies may reflect interannual variation in jellyfish biomass or changes in the overlap with fisheries. Abundant jellyfish may have a negative impact on fishes as they compete with planktivorous fishes for prey resources (Purcell and Sturdevant 2001), and additionally, jellyfish may prey upon the early life history stages (eggs and larvae) of fishes (Purcell and Arai 2001, Robinson et al. 2014).

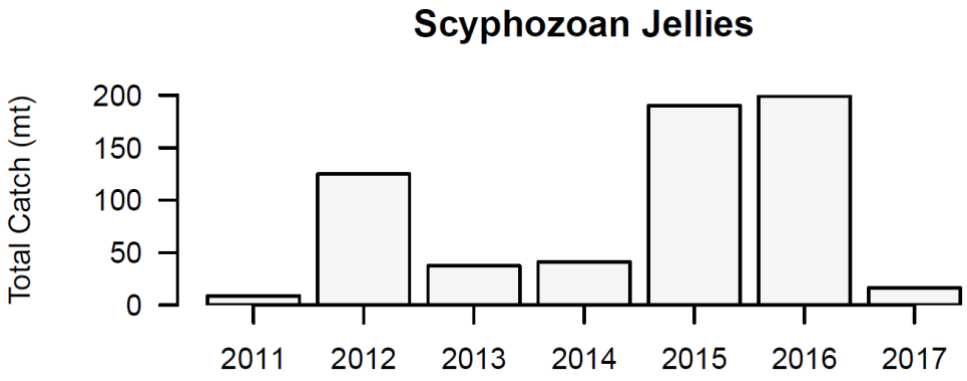

Figure R12-17. Total catch of Scyphozoan jellyfish (tons) obtained by GOA groundfish fisheries (2011–2017).

6.5. Jellyfish in Trawl Surveys

Investigator: Chris Rooper
NOAA Alaska Fisheries Science Center
Source: GOA ESR 2017

Methods: RACE bottom trawl surveys in the Gulf of Alaska (GOA) are designed primarily to assess populations of commercially important fish and invertebrates. However, many other species are identified, weighed and counted during the course of these surveys and these data may provide a measure of relative abundance for some of these species. Jellyfish are probably not sampled well by the gear due to their fragility and potential for catch in the mid-water during net deployment or retrieval. Therefore, jellyfish encountered in small numbers which may or may not reflect their true abundance in the GOA. The fishing gear used aboard the Japanese vessels that participated in all GOA surveys prior to 1990 was very different from the gear used by all vessels since. This gear difference almost certainly affected the catch rates for jellyfish. For jellyfish, the catches for each year were scaled to the largest catch over the time series (which was arbitrarily scaled to a value of 100). The standard error (+/- 1) was weighted proportionally to the CPUE to get a relative standard error. The percentage of positive catches in the survey bottom trawl hauls was also calculated.

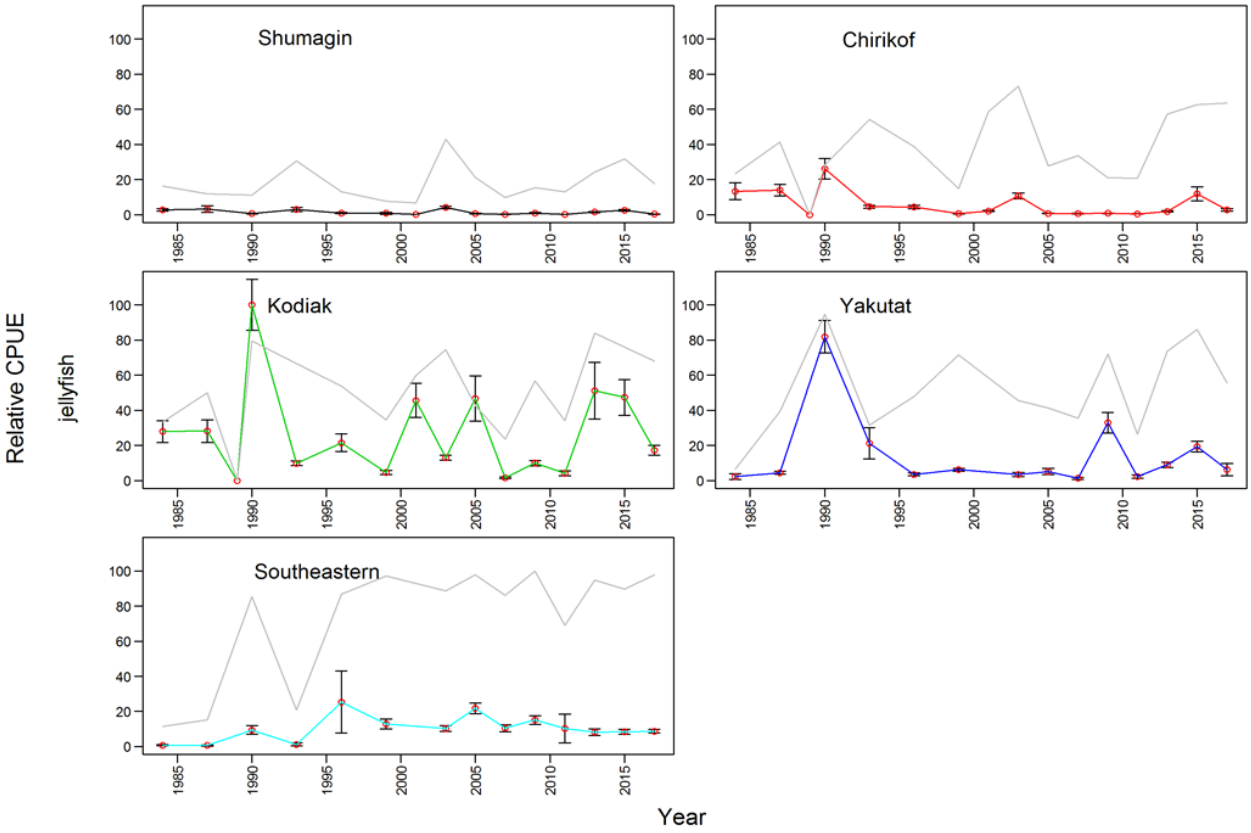

Figure R12-18. Relative mean CPUE of jellyfish species by area from RACE bottom trawl surveys in the Gulf of Alaska from 1984 through 2017. Error bars represent standard errors. The gray lines represent the percentage of non-zero catches.

Trends: Biennial survey results show very few trends in jellyfish abundance across time, with most of the trends being consistent within regions (Figure R12-18). Jellyfish mean catch per unit effort (CPUE) is typically higher in the Kodiak region than in other areas. The frequency of occurrence in trawl catches is generally high across all areas, except the Shumagins, but has been variable. Jellyfish catches in the western GOA (Chirikof and Shumagin areas) have been uniformly low. Jellyfish catch in the Kodiak area decreased from peaks during the 2013 and 2015 surveys. Jellyfish catches in the eastern GOA (Yakutat and Southeastern areas) have been low.

7. Fishes and Invertebrates

7.1. Forage fish indicators

Investigator: Stephani Zador
NOAA Alaska Fisheries Science Center
Source: GOA ESR 2016

Methods: The North Pacific Fisheries Management Council currently monitors trends in the abundance of capelin using an index based on prey composition of various piscivorous seabird and groundfish. Time series of capelin and sand lance data from each predator were analyzed using dynamic factor analysis (DFA). Similar to a principal component analysis, DFA reduces multiple time series into fewer common trends. The resulting factors in the best fit models were considered to represent trends in the relative abundance of capelin and sand lance. Prey data are from seabird chick diets collected at breeding colonies during summer by the U.S. Fish and Wildlife Service (USFWS) and Institute for Seabird Research and Conservation, and from groundfish stomach contents collected biennially during summer bottom trawl surveys and maintained in NOAA's Resource Ecology and Ecosystem Modeling Food Habits database (https://www.afsc.noaa.gov/REFM/REEM/data/default.htm). The data include the percent diet composition from tufted puffins (*Fratercula cirrhata*, TUPU) and common murres (*Uria aalge*, COMU) at East Amatuli Island (USFWS), relative prey occurrence during June to August in black-legged kittiwakes (*Rissa tridactyla*, BLKI) and percent biomass from the diet of rhinoceros auklets (*Cerorhinca monocerata*, RHAU) at Middleton Island (ISRC), and the number of capelin per length of groundfish. The groundfish species included arrowtooth flounder (*Atherestes stomias* ATF), Pacific cod (*Gadus macrocephalus*, COD), Pacific halibut (*Hippoglossus stenolepis*, HAL), and pollock (*Gadus chalcogramma*, POL).

Trends (Figure R12-19): The capelin DFA supports a single trend model. Four of the prey data series load strongly and positively onto the trend. These include rhinoceros auklets, Pacific cod, black-legged kittiwakes, and Pacific halibut. Capelin abundance was low in 1998 and 2003–2005. Abundance increased sharply in 2007, then decreased in 2014/2015. The increase in abundance coincides with the cooler years. Abundance dropped off at the same time that the marine heatwave began. The sand lance DFA also supported a single trend model. Sand land abundance decreased in the mid-90s before becoming abundant again. A longer period of decline began in 2000, and abundance has remained at the lowest in the time series from 2011–2015. Five of the prey data series, particularly of diet composition of tufted puffins, load strongly and positively onto the trend.

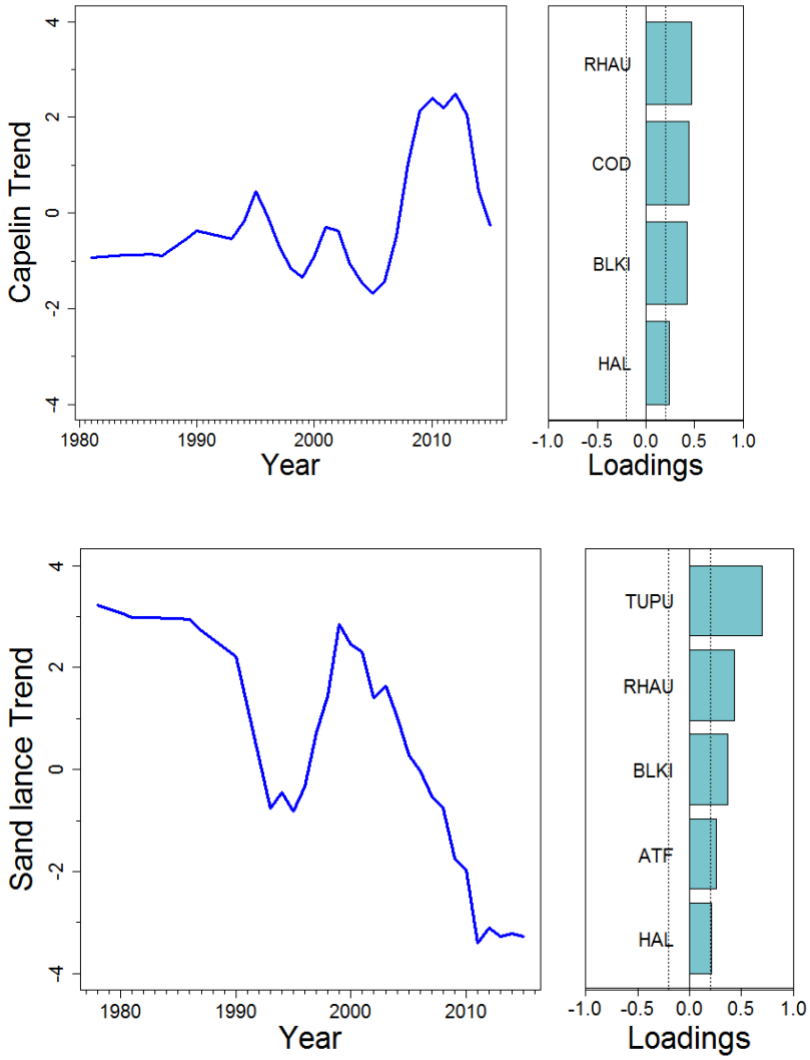

Figure R12-19. Trends from the best-fit capelin (top) and sand lance (bottom) DFAs indicating temporal trends in abundance (left) and the predator time series that loaded most strongly onto those trends (right). RHAU: rhinoceros auklets, TUPU: tufted puffins, COMU: common murres, BLKI: black-legged kittiwakes, COD: Pacific cod, ATF: arrowtooth flounder, HAL: Pacific halibut.

7.2. Aggregated Catch-Per-Unit-Effort of Fish and Invertebrates in Bottom Trawl Surveys in the Gulf of Alaska, 1993-2017

Investigator(s): Franz Mueter
University of Alaska
Source: GOA ESR 2017

Methods: This index provides a measure of the overall biomass of benthic, demersal, and semi-demersal fish and invertebrate species. We obtained catch-per-unit-effort (CPUE in kg ha^{-1}) of

fish and major invertebrate taxa for each successful haul completed during standardized bottom trawl surveys on the Gulf of Alaska shelf (GOA), 1993–2017. Total CPUE for each haul was computed as the sum of the CPUEs of all fish and invertebrate taxa. To obtain an index of average CPUE by year, we modeled log-transformed total CPUE (N = 6333 and 1561 hauls in the western and eastern GOA, respectively) as smooth functions of depth, alongshore distance and sampling stratum with year-specific intercepts using Generalized Additive Models following Mueter & Norcross (2002). Hauls were weighted based on the area represented by each stratum. To avoid biases due to gear and vessel issues, data prior to the 1993 survey was not included in the analysis.

Trends: Total log(CPUE) in both the eastern and western GOA decreased from its highest value in 2013 to its lowest value in 2017 (Fig. R12-20). There was no significant long-term trend over time from 1993 to 2017 in either region, but total CPUE decreased significantly and by more than 50% between 2013 to 2017 in both regions. The drop in CPUE since 2013 was widespread among species with over 2/3 of the species in both the eastern and western GOA showing declines from 2013 to 2017. Large declines were observed in arrowtooth flounder, walleye pollock, and Pacific ocean perch in both regions; northern rockfish, grenadiers, rock sole and Atka mackerel in the western GOA; and shortraker rockfish, spiny dogfish, Pacific halibut, Dover sole, and dusky rockfish in the eastern GOA.

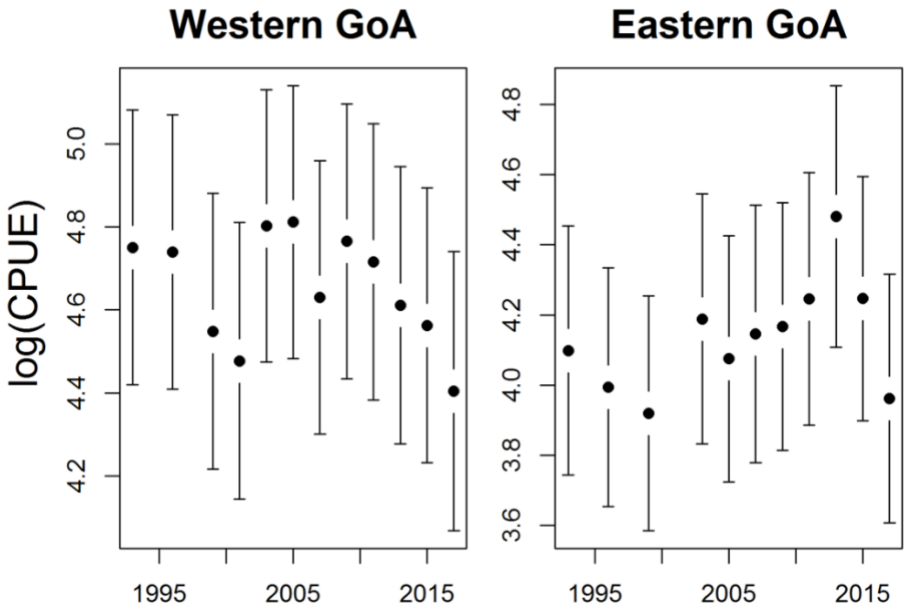

Figure R12-20. Model-based estimates of total log(CPUE) for major fish and invertebrate taxa captured in bottom trawl surveys from the western (west of 147°W) and eastern Gulf of Alaska by survey year (1993-2017) with approximate 95% confidence intervals. Estimates were adjusted for differences in depth and sampling locations (alongshore distance) among years. No sampling in the eastern Gulf of Alaska in 2001.

7.3. Biomass in trawl surveys aggregated by foraging guild

Investigator(s): Stephani Zador, Andy Whitehouse
NOAA Alaska Fisheries Science Center
Source: GOA ESR 2017

Methods: The NOAA bottom trawl survey has been conducted triennially since 1984, and biennially since 2000. The next survey will be in 2019. Foraging guild biomass is calculated from the survey data modified by an Ecopath-estimated catchability. Here we show aggregated biomass west of 144º W. Fish in the apex predator guild include: Pacific cod, arrowtooth flounder, halibut, sablefish, large sculpins, and skates. Marine mammals, seabirds, and some other fishes such as sharks are included as constant Ecopath-estimated biomasses. Fish in the pelagic forager guild include: walleye pollock, herring, Atka mackerel, capelin, sand lance, and eulachon. Fish in the benthic forager guild include: small flatfish such as yellowfin and flathead sole, and juvenile cod, arrowtooth flounder, and halibut.

Trends (FigureR12-21): The steep decline in apex predator biomass in 2017 reflects declines in Pacific cod, arrowtooth flounder, and halibut. Apex predator biomass was already low in 2013 and 2015. The marine heatwave appeared to cause high natural mortality for cod.

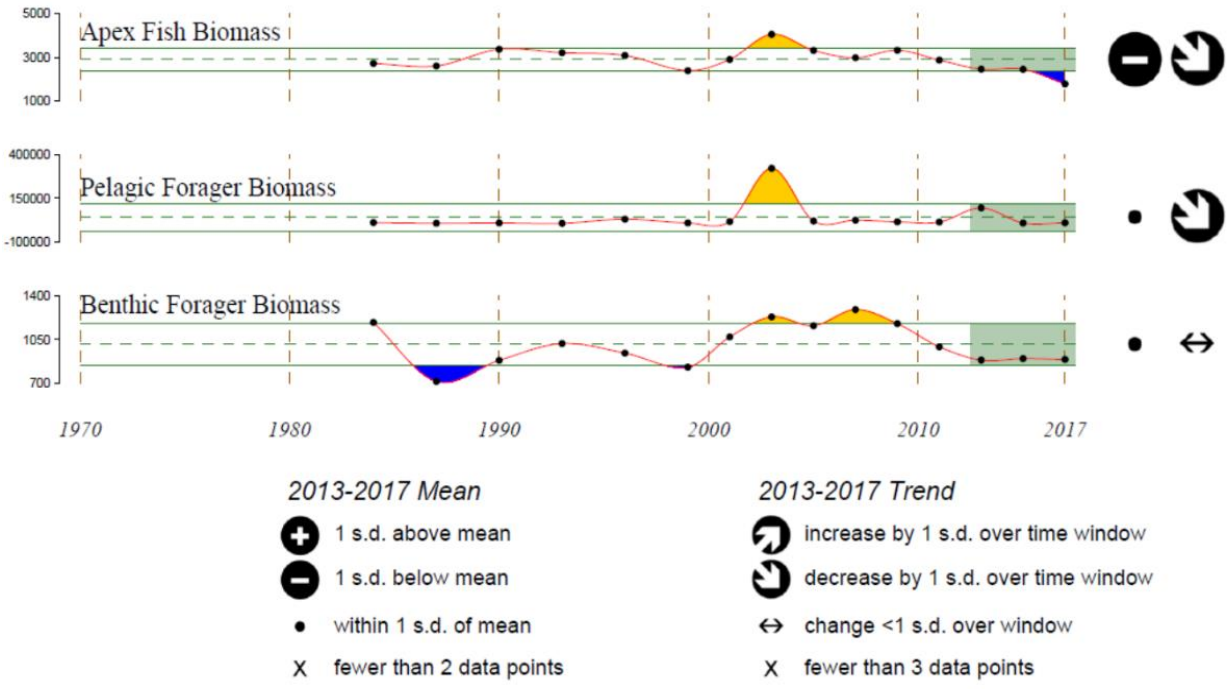

Figure R12-21. Time-series fish biomass in NOAA trawl surveys in the western Gulf of Alaska 1984-2017 aggregated by foraging guild and standardized over the time series. Broken and solid green lines indicate the overall mean and 1 x SD. Symbols on right indicate the 2014-2018 trend and the extent of the 2014-2018 mean relative to the 1984-2017 mean.

7.4. Groundfish Condition in Bottom Trawls

Investigator(s): Jennifer Boldt, Chris Rooper, Jerry Hoff
NOAA Alaska Fisheries Science Center
Source: GOA ESR 2017, ETSO

Methods: Length-weight residuals are an indicator of somatic growth (Brodeur et al. 2004) and, therefore, a measure of fish condition. Fish condition is an indicator of how heavy a fish is per unit body length, and may be an indicator of ecosystem productivity. Positive length-weight residuals indicate fish are in better condition (i.e., heavier per unit length); whereas, negative residuals indicate fish are in poorer condition (i.e., lighter per unit length). Fish condition may affect fish growth and subsequent survival (Boldt and Haldorson 2004). The AFSC Gulf of Alaska bottom trawl survey data was utilized to acquire lengths and weights of individual fish for walleye pollock, Pacific cod, arrowtooth flounder, southern rock sole, dusky rockfish, northern rockfish, and Pacific ocean perch. Only standard survey stations were included in analyses. Data were combined by all International North Pacific Fisheries Commission (INPFC) area; Shumagin, Chirikof, Kodiak, Yakutat and Southeastern. Length-weight relationships for each of the seven species were estimated with a linear regression of log-transformed values over all years where data were available (during 1985-2017). Additionally, length-weight relationships for age 1+ walleye pollock (length from 100-250 mm) were also calculated independent from the adult life history stage. Predicted log-transformed weights were calculated and subtracted from measured log-transformed weights to calculate residuals for each fish. Length-weight residuals were averaged for the entire GOA and for the 5 INPFC areas sampled in the standard summer survey. Temporal patterns in residuals were examined.

Trends: Length-weight residuals varied over time for all species with a few notable patterns. In general, for all species except the gadids (pollock and cod), there has been a general decrease in body condition since 1990 for most species where there was data were positive in the first three years of the survey (1985-1990) (Figure R12-22). The residuals have been mixed for all species since then, generally smaller and varying from year to year. Age-1 pollock have generally been at or near the mean condition since the 1990 survey (although 2017 was a negative condition year). In 2017 condition was reduced from the average for all species except Pacific cod. Fish condition for northern rockfish and arrowtooth flounder was the lowest on record and Pacific Ocean perch and southern rock sole were the second lowest on record.

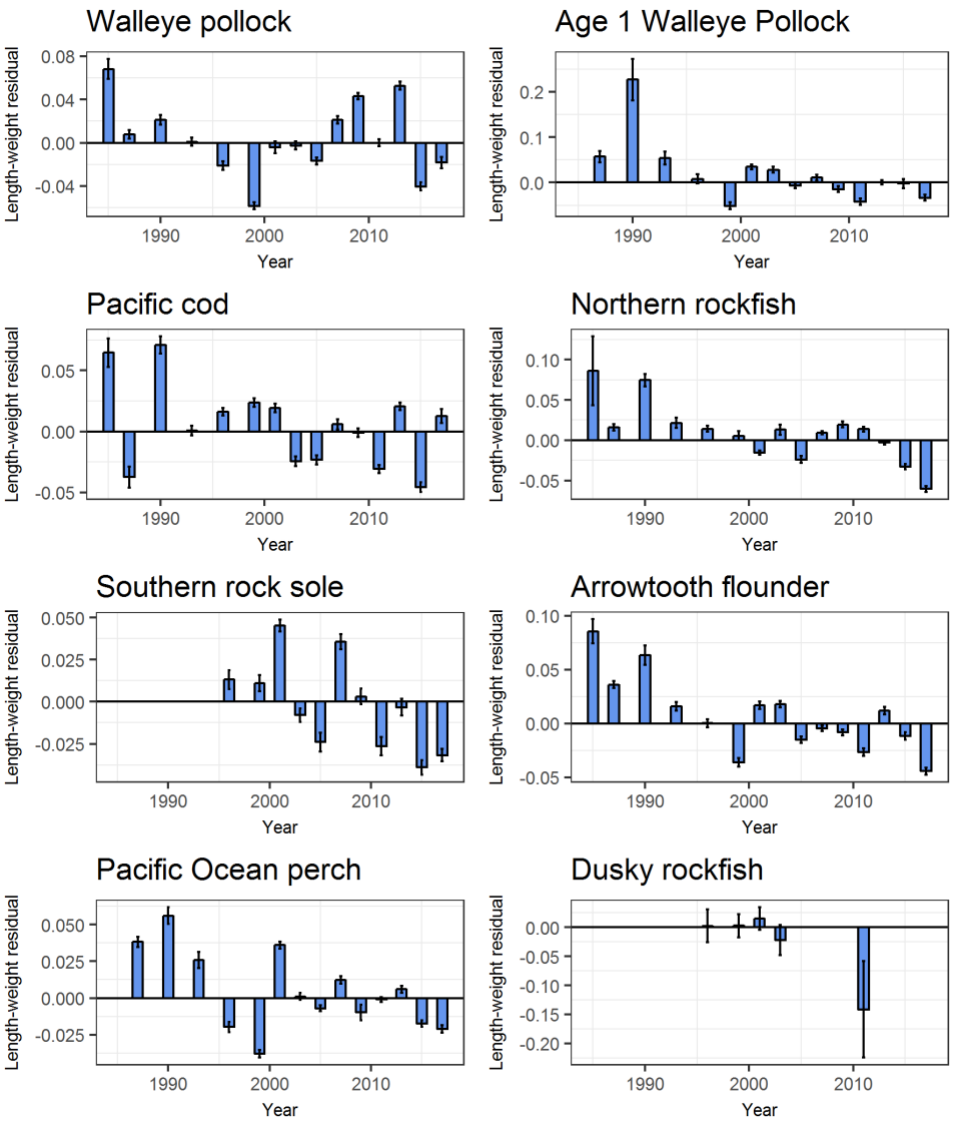

Figure R12-22. Length-weight residuals for seven Gulf of Alaska groundfish sampled in the NMFS standard summer bottom trawl survey, 1985-2017.

7.5. Distribution of Rockfish Species along Environmental Gradients in Gulf of Alaska and Aleutian Islands Bottom Trawl Surveys

Investigator(s): Chris Rooper
NOAA Alaska Fisheries Science Center
Source: GOA ESR 2017, ETSO

Methods: In this time-series, the mean-weighted distributions of six rockfish (five *Sebastes* spp. and *Sebastolobus alascanus*) species along the three environmental gradients (depth, temperature, and distance from Hinchinbrook Island, Alaska) were calculated for the Gulf of Alaska. A weighted mean value for each environmental variable was computed for each survey. The weighted standard error (SE) was then computed. Details of the calculations and analyses

can be found in Rooper (2008). These indices monitor the distributions of major components of the rockfish fisheries along these environmental gradients to detect changes or trends in rockfish distribution.

Trends: In the Gulf of Alaska, there continue to be no significant trends in the distribution of rockfish with depth, temperature and position (Figure R12-23). This is in contrast to some of the earlier years in which the indicator was calculated. The distribution of rockfish species in the bottom trawl surveys appears to have stabilized for the Gulf of Alaska. In the Gulf of Alaska, the stability of the distribution indicates that each of the species occupies a fairly specific depth distribution. This is seen in the flat line time series of distribution across depths and the variability in temperature. As temperatures rise and fall around the mean, the depth distribution does not change, indicating that the rockfish are not changing their habitat or distribution to maintain a constant temperature.

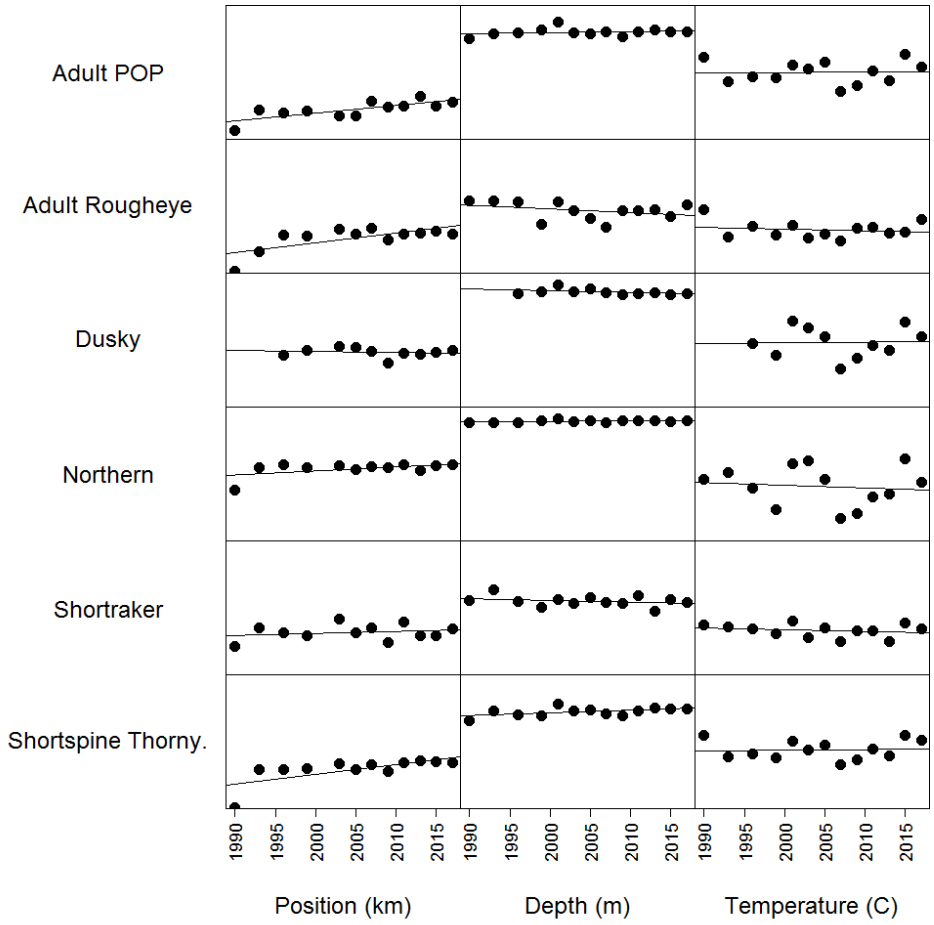

Figure R12-23. Plots of mean weighted (by catch per unit effort) distributions of six rockfish species-groups along three environmental variables in the Gulf of Alaska. Mean weighted distributions of rockfish species-groups are shown for position (left), depth (middle), and temperature (right). Position is the distance from Hinchinbrook Island, Alaska, with higher values indicates west of this central point in the trawl surveys and lower values in southeastward.

7.6. Pink salmon abundance (hatchery-origin plus natural-origin)

Investigator: Gregory Ruggerone, Jim Irvine
Source: ETSO

Methods: Data include the south side of the Alaska Peninsula, Kodiak, Cook Inlet, Prince William Sound, and Southeast Alaska regions. See Ruggerone and Irvine (2018) for the details.

Trends: Strong biennial cycles are evident, as well as the record runs in 2013, and high runs in 2015 and 2017 (not shown) as well (Figure R12-24)

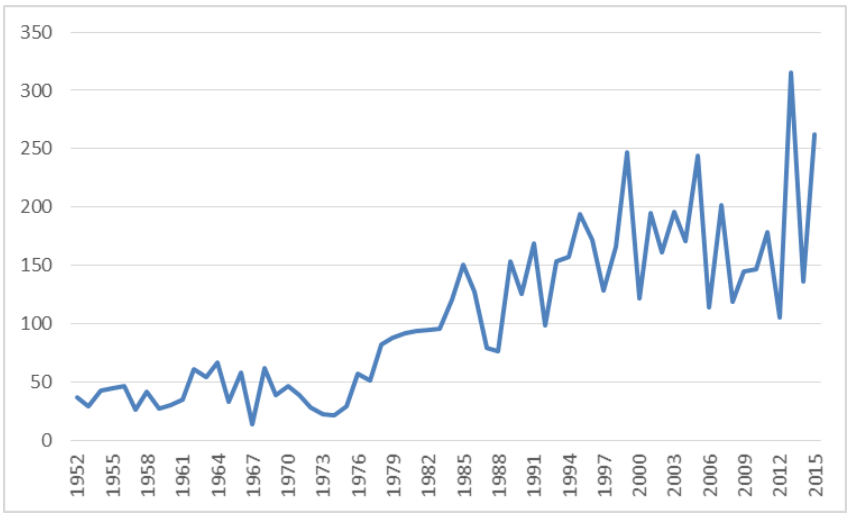

Figure R12-24. Pink salmon (hatchery-origin plus natural-origin) abundance (number of catch and escapement in millions of fish). Data from Ruggerone and Irvine (2018).

8. Biogenic Habitat (e.g. eelgrass, coral)

Note: There was one ETSO submitted, but the investigator noted that the data were not a good indicator of trends, so we chose not to include it here.

9. Marine Birds

9.1. Reproductive Success of Seabirds in the Gulf of Alaska

Investigator(s): Heather Renner, Nora Rojek, Arthur Kettle, Brie Drummond
US Fish and Wildlife Service
Source: GOA ESR 2018

Methods: The Alaska Maritime National Wildlife Refuge has monitored seabirds at colonies around Alaska in most years since the early- to mid-1970s. Time series of annual breeding success and phenology (and other parameters) are available from over a dozen species at eight Refuge sites in the Gulf of Alaska, Aleutian Islands, and Bering and Chukchi Seas. Monitored colonies in the Gulf of Alaska include Chowiet (Semidi Islands), East Amatuli (Barren Islands), and St. Lazaria (Southeast Alaska) islands. Reproductive success is defined as the proportion of nest sites with eggs (or just eggs for murres that do not build nests) that fledged a chick.

Trends (Figure R12-25): Fish-eating seabirds in the Gulf of Alaska had generally normal reproductive success in 2018. Common murres, which showed rare widespread reproductive failure in 2015–2016, and improved success in 2017, generally had yet better colony attendance and fledging rates in 2018; still the number of birds breeding was low at most sites. Tufted puffin productivity was within 1 standard deviation (SD) of the long-term mean at all monitored sites. Black-legged kittiwakes and storm-petrels (which consume a mix of fish and invertebrates) showed fledging rates within 1 SD of the mean; success of planktivorous auklets was low at Chowiet. Timing of breeding was normal for most species at Chowiet, late for murres at E Amatuli, and late for murres and gulls at St. In general, murres appear to have been negatively affected during the marine heat wave of 2015–2016, with widespread reproductive failures, die-offs, and low attendance at breeding colonies. Murre attendance is still lower than prior to the heat wave, but improvements in reproductive success in 2018 suggest environmental changes have returned back to more neutral conditions. Other species did not show broad-scale failures during this period; planktivorous seabirds were generally successful; however, planktivorous auklets did poorly at Chowiet in 2018.

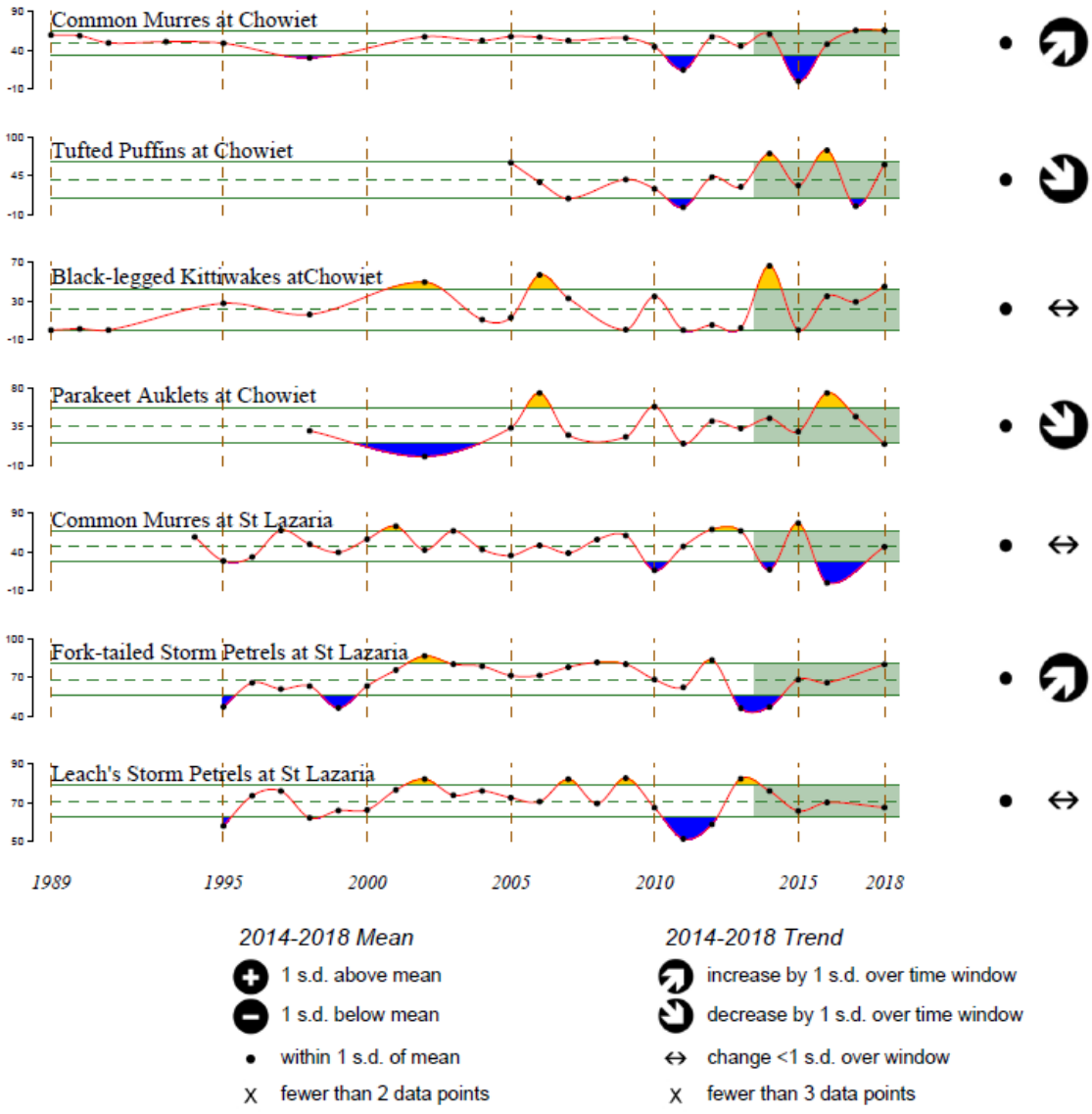

Figure R12-25. Reproductive success of seabirds at Chowiet Island (western Gulf of Alaska) and St. Lazaria Island (eastern Gulf of Alaska). Broken and solid green lines indicate the overall mean and 1 x SD. Symbols on right indicate the 2014-2018 trend and the extent of the 2014-2018 mean relative to the overall mean.

10. Marine Mammals

10.1. Steller Sea Lions in the Gulf of Alaska

Investigators: Katie Sweeney, Tom Gelatt
NOAA Alaska Fisheries Science Center
Source: GOA ESR 2018

Methods: The Marine Mammal Laboratory (MML) uses the R package agTrend to model Steller sea lion (SSL) non-pup and pup counts and trend estimates (an index of population abundance and trends) within the bounds (Distinct Population Segment: DPS) of the Gulf of Alaska (Figure R12-26).

Trends: Non-pup steller sea lion abundance in the western DPS in the GOA began to decline in the late-1970s, with the steepest decline occurring in the mid-to late-1980s, until it leveled out in 2001 and began to gradually increase an average of 3.47% per year (95%CI 2.64 – 4.34%; Merrick et al. 1987, Fritz et al. 2016; Figure R12-27). Between 1978 and 2017, the western DPS abundance has declined an average 2.84% per year (95% CI 3.14 – 2.54%). The survey counts from the most recent surveys of this region in 2015 and 2017 indicated that number of non-pups remained stable, despite having increased between 2001 and 2013 (Sweeney et al. 2017). Concurrently, 2017 pup counts in the eastern and central DPSs declined from 2015 counts by 33 and 18%, respectively (Sweeney et al. 2017). Since regular surveys began in the eastern DPS in the early 1970s, southeast Alaska Steller sea lion abundance has been steadily increasing (Fritz et al. 2016). Between 1971 and 2017, the abundance in the eastern DPS increased 2.21% per year (95% CI 1.55 – 2.84%; Figure R12-28). Since 2013, the non-pup and pup count estimates appear to be oscillating around an apparent carrying capacity. However, more years of data are necessary to distinguish these changes from potential declines (Sweeney et al. 2017).

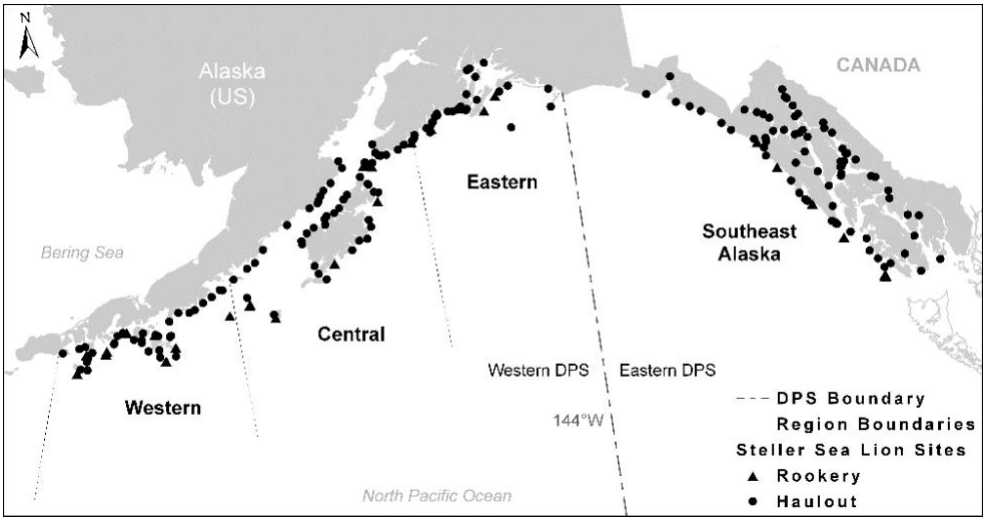

Figure R12-26. Steller sea lion regions (Distinct Population Segment: DPS) in the Gulf of Alaska.

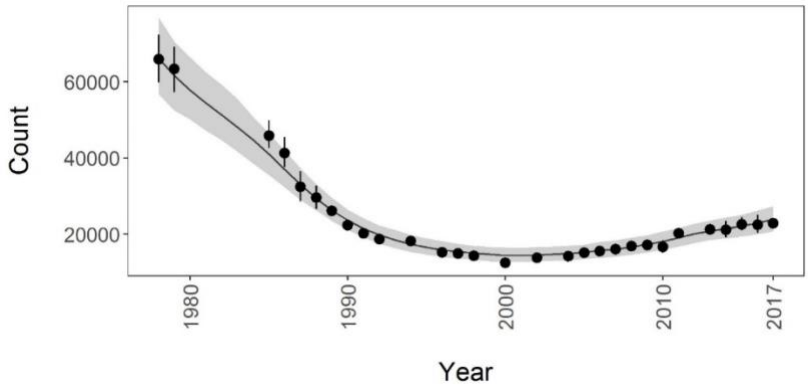

Figure R12-27. Steller sea lion non-pup count estimate in the western DPS in the Gulf of Alaska.

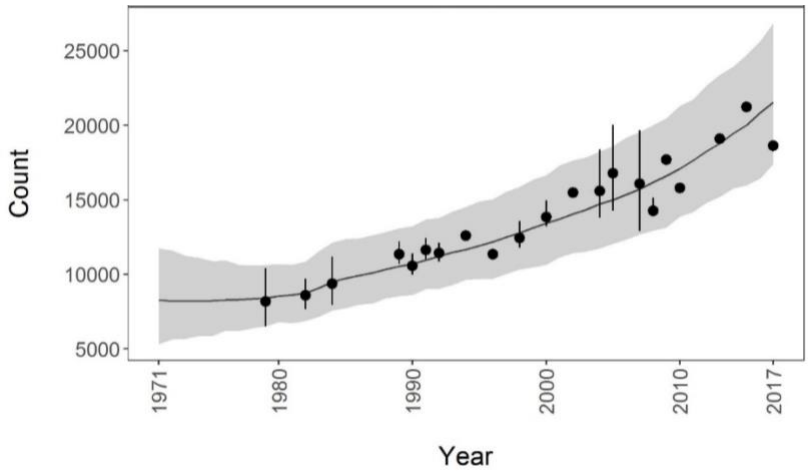

Figure R12-28. Steller sea lion non-pup count estimate in the eastern DPS in the Gulf of Alaska.

10.2. Large whale Unusual Mortality Events (UMEs)

Investigator: K. Savage
Source: Savage, K. 2017. Alaska and British Columbia Large Whale Unusual Mortality Event Summary Report. Protected Resources Division, NOAA Fisheries, Juneau, AK

Methods: see Savage (2017) for the details.

Trends: An Unusual Mortality Event was declared for large whales in the Gulf of Alaska from April 23, 2015, to April 16, 2016 (Table R12-1). Humpback whales are one of the most common marine mammal species reported stranded in Alaska, and the most common large cetacean species. Approximately 61% of the 2010 – 2014 humpback whale reports were from carcasses observed in the GOA (range 50 – 75%). In 2015, 25 dead humpback whales were reported from the GOA, which decreased to 9 whales in 2016. In 2015, 13 dead fin whales were reported stranded in the GOA and south-central Alaska while it decreased to 2 in 2016 (figure R12-29).

Year	Number of Confirmed Reports by Species			
	Fin whale	Humpback whale	Gray whale	Unidentified whale
2000	0	2	45 (?)	5
2001	0	8	5	1
2002	0	1	0	4
2003	2	1	4	3
2004	0	2	1	6
2005	0	13	5	4
2006	1	5	8	7
2007	0	2	2	6
2008	0	19	6	8
2009	1	3	10	14
2010	1	16	15	13
2011	0	12	9	5
2012	1	12	23	28
2013	1	15	10	10
2014	2	8	13	9
2015	14	31	17	22
2016	3	19	17	22

Table R12-1. Number of confirmed large whale mortalities by species throughout Alaska.

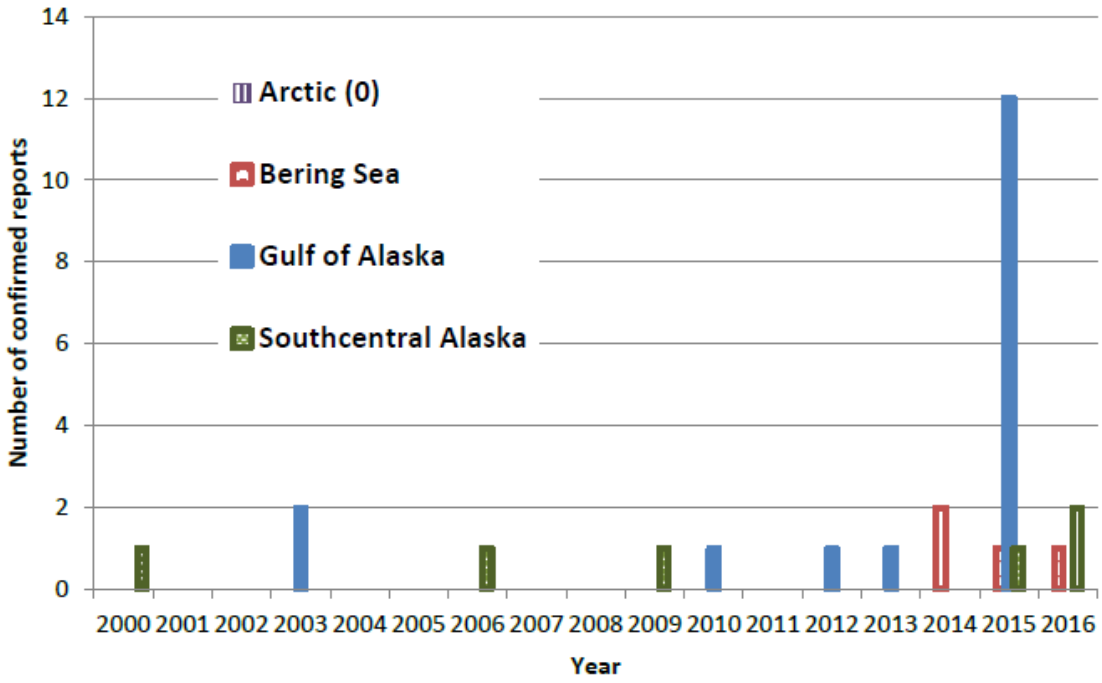

Figure R12-29. Number of confirmed reports of dead fin whales by regional subarea.

11. Pollutants/Contaminants

11.1. Trends of Brominated Flame Retardants (BFR) in marine birds from the Pacific coast of Canada: 1990–2015

Investigator(s): John E. Elliott, Aroha A. Miller, Kyle H. Elliott, Sandi Lee
Environment and Climate Change Canada, Ecotoxicology and Wildlife Health Directorate, Pacific Wildlife Research Centre, Delta, BC, Canada, V4K 3N2
Source: ETSO

Methods: Detailed methods are described in Miller et al. (2014), including basic biology of study species, study locations, egg collection, and analytic methods. Briefly, 15 eggs were collected at four-year intervals from randomly selected nests at the monitoring colonies and transported to the laboratory. Five pools were prepared consisting of three whole eggs each, and analyzed by gas chromatography with a mass specific detector (GC/MSD), with appropriate quality assurance procedures. ∑PBDEs consisted of 14 congeners (17, 28, 47, 49, 66, 85, 99, 100, 138, BDE 154/BB 153, 153, 183, 190, 209), with dominant congeners being BDEs, 47, 99 and 100. For purposes of this PICES status and trends report, we selected data for two species and locations: storm-petrels from Hippa Island (53°26'N 132°59'W), located on the northwest of Haida Gwaii in the Gulf of Alaska, and rhinoceros auklets from Cleland Island (49°10'N; 126° 5'W) off the south-central west coast of Vancouver Island.

Trends: Following implementation of voluntary restrictions by North American industry and subsequent phase out of penta-BDE mixtures, ΣPBDE concentrations generally decreased in rhinoceros auklet eggs from the colony at Cleland Island (Figure R12-30 bottom). However, that trend was not apparent for storm-petrel eggs collected at Hippa Island, although the doubling time did decline post-2000 (Figure R12-30 top). That particular trend in PBDEs in storm-petrels from Hippa Island may be the result of that breeding population foraging farthest from North America and closest to Asia. Among the colonies monitored here, Hippa Island is the most distal from any influence of coastal industrial activity. As a result, the impact of regulatory changes on contaminant release could be delayed in birds breeding at remote sites, which could explain the lower exposure to PBDEs detected in Hippa Island storm-petrels.

As we reported previously, there were no significant temporal trends in δ15N and δ13C in eggs of either species (Miller et al., 2014). Thus there was no indication of any temporal shifts in trophic level (δ15N) influencing ΣPBDE for individual species and sites, although spatial variation determined from carbon source (δ13C) had to be accounted for. Those stable isotope data indicate that diet was stable over time, and therefore there was no detected effect of trophic level at this scale. Thus, the temporal trends in BFRs reported here are likely not caused by dietary factors and instead are almost certainly due to restrictions imposed on PBDE usage (Canadian Gazette, 2006: https://gazette.gc.ca/rp-pr/p1/2022/2022-05-14/html/reg2-eng.html).

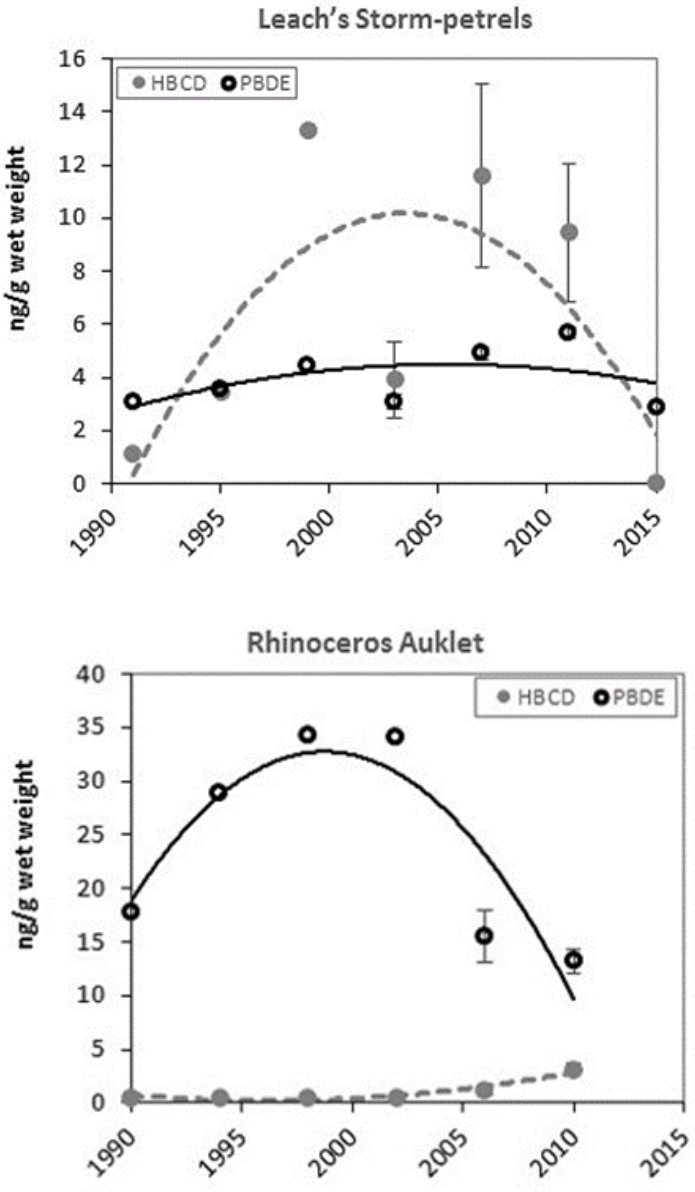

Figure R12-30 HBCDD and ∑PBDE (ng/g lw) over time in Leach's storm-petrel eggs from Hippa Island (top); Rhinoceros auklet eggs from Cleland Island (bottom). Standard error of the mean is shown in years where multiple pooled samples were taken; Adapted from Miller et al. 2014.

References

Boldt, J.L. and Haldorson, L.J. (2004) Size and condition of wild and hatchery pink salmon juveniles in Prince William Sound, Alaska. Transactions of American Fisheries Society 133: 173-184.

Brodeur RD, Decker MB, Ciannelli L, Purcell JE, Bond NA, Stabeno PJ, Acuna E, Hunt GL (2008) Rise and fall of jellyfish in the eastern Bering Sea in relation to climate regime shifts. Progress in Oceanography 77:103-111. doi:10.1016/j.pocean.2008.03.017

Chiba, S., E. Di Lorenzo, A. Davis, J. E. Keister, B. Taguchi, Y. Sasai, and H. Sugisaki (2013) Large-scale climate control of zooplankton transport and biogeography in the Kuroshio-Oyashio Extension region, Geophys. Res. Lett., 40, 5182–5187, doi:10.1002/grl.50999.

Chu, P. C., Q. Q. Wang, R. H. Bourke (1999) A geometric model for Beaufort/Chukchi Sea thermohaline structure. J Atmos OceanTechnol ,16:613–632.

Di Lorenzo, E. and Co-Authors (2008): North Pacific Gyre Oscillation links ocean climate and ecosystem change. Geophys. Res. Lett., 35, doi:10.1029/2007GL032838.

Doyle, M. J., Picquelle, S. J., Mier, K. L., Spillane, M. C., & Bond, N. A. (2009). Larval fish abundance and physical forcing in the Gulf of Alaska, 1981–2003. *Progress in Oceanography*, *80*(3-4), 163-187.

Fritz, L., K. Sweeney, R. Towell, and T. Gelatt. 2016. Aerial and ship-based surveys of Steller sea lions (Eumetopias jubatus) conducted in Alaska in June-July 2013 through 2015, and an update on the status and trend of the western distinct population segment in Alaska. U.S. Dep. Commer., NOAA Tech. Memo. NMFS-AFSC-321, 72 p.

Hobday, A.J., Alexander, L.V., Perkins, S.E., Smale, D.A., Straub, S.C., Oliver, E.C., Benthuysen, J.A., Burrows, M.T., Donat, M.G., Feng, M. and Holbrook, N.J., 2016. A hierarchical approach to defining marine heatwaves. Progress in Oceanography, 141, pp.227-238.Mantua, N.J., S.R. Hare, Y. Zhang, J.M. Wallace, and R.C. Francis (1997): A Pacific interdecadal climate oscillation with impacts on salmon production. Bull. Amer. Meteor. Soc., 78, pp. 1069-1079.

Matarese, A. C. (2003). *Atlas of abundance and distribution patterns of ichthyoplankton from the northeast Pacific Ocean and Bering Sea ecosystems based on research conducted by the Alaska Fisheries Science Center (1972-1996)* (Vol. 1). US Department of Commerce, National Oceanic and Atmospheric Administration, National Marine Fisheries Service.

Merrick, R. L., T. R. Loughlin, and D. G. Calkins. 1987. Decline in abundance of the northern sea lion, Eumetopias jubatus, in 1956-86. Fish. Bull., U.S. 85:351-365.

Miller AA, Elliott JE, Elliott KH, Guigueno MF, Wilson LK, Lee S, Idrissi A. 2014. Spatial and Temporal trends in Brominated Flame Retardants in Seabirds from the Pacific Coast of Canada Environmental Pollution. 195: 48-55. Doi: 10.1016/j.envpol.2014.08.009.

Mueter, F.J., and B.L. Norcross. 2002. Spatial and temporal patterns in the demersal fish community on the shelf and upper slope regions of the Gulf of Alaska. Fish. Bull. 100(3): 559-581.

Newman, M. and Co-Authors (2016): The Pacific Decadal Oscillation, Revisited. J. Climate, doi.org/10.1175/JCLI-D-150508.1

Purcell JE (2005) Climate effects on formation of jellyfish and ctenophore blooms: a review. Journal of the Marine Biological Association of the United Kingdom 85:461-476. doi:10.1017/s0025315405011409

Purcell JE, Arai MN (2001) Interactions of pelagic cnidarians and ctenophores with fish: a review. Hydrobiologia 451:27-44. doi:10.1023/a:1011883905394

Purcell JE, Sturdevant MV (2001) Prey selection and dietary overlap among zooplanktivorous jellyfish and juvenile fishes in Prince William Sound, Alaska. Mar Ecol-Prog Ser 210:67-83. doi:10.3354/meps210067

Robinson KL, Ruzicka JJ, Decker MB, Brodeur RD, Hernandez FJ, Ouinones J, Acha EM, Uye S, Mianzan H, Graham WM (2014) Jellyfish, Forage Fish, and the Worlds Major Fisheries.

Rooper, C.N. 2008. An ecological analysis of rockfish (*Sebastes* spp.) assemblages in the North Pacific Ocean along broad-scale environmental gradients. Fish. Bull. 106:1-11.

Ruggerone, G.T. and Irvine, J.R., 2018. Numbers and biomass of natural-and hatchery-origin pink salmon, chum salmon, and sockeye salmon in the North Pacific Ocean, 1925–2015. Marine and Coastal Fisheries, 10(2), pp.152-168.

Savage, K. (2017). Alaska and British Columbia large whale unusual mortality event summary report.

Schlegel, R. W., & Smit, A. J. (2018). heatwaveR: A central algorithm for the detection of heatwaves and cold-spells. *Journal of Open Source Software*, *3*(27), 821.

Strom, S. L., Olson, M. B., Macri, E. L., & Mordy, C. W. (2006). Cross-shelf gradients in phytoplankton community structure, nutrient utilization, and growth rate in the coastal Gulf of Alaska. *Marine Ecology Progress Series*, *328*, 75-92.

Sweeney, K. L., L. Fritz, R. Towell, and T. Gelatt. 2017. Results of Steller sea lion surveys in Alaska, June-July 2017. Memorandum to The Record, November 29, 2017. https://www.afsc.noaa.gov/NMML/PDF/SSL_Aerial_Survey_2017.pdf

Trenberth, K.E. and J.W. Hurrell (1994): Decadal Atmospheric-Ocean Variations in the Pacific. Climate Dynamics, 9, 303-319, doi.org/10.1007/BF00204745

Wong et al., 2015, Argo quality control manual for CTD and trajectory data Version 3.0, http://dx.doi.org/10.13155/33951